공학박사학위논문

전륜 구동 차량의 핸들링 성능을 위한 전자식 차동 제한 장치의 예측 제어 전략

A Predictive Control Strategy for Handling Performance of Front-Wheel-Drive Vehicles with Electronic Limited Slip Differential

2020 년 8월

서울대학교 대학원

기계항공공학부

우 승 훈

Abstract

A Predictive Control Strategy for Handling Performance of Front-Wheel-Drive Vehicles with Electronic Limited Slip Differential

Seunghoon Woo

School of Mechanical and Aerospace Engineering

The Graduate School

Seoul National University

This dissertation focused on a predictive control strategy for improved handling and acceleration performance of front-wheel-drive vehicles with electronic limited slip differential. Conventional front-wheel-drive cars have certain disadvantages, including a lack of accelerating performance and excessive understeer during acceleration in turn, due to the fact that spin of the inner driving wheel can occur with a small vertical load on the wheel. To address this problem, control logic is proposed for an electronic limited slip differential (ELSD) to enhance handling and acceleration performance. The proposed ELSD control algorithm consists of four parts. (1) Understeer prevention logic is developed for acceleration in turn. First, for a rapid response, the driving torque is distributed in advance to the inner and outer wheels according to the magnitude of the estimated traction potential in the wheels. If wheel spin occurs because of insufficient inner grip, then additional driving torque is transmitted to the outer wheel in proportion to the increment of the inner wheel speed compared to the outer wheel. However, the torque transfer to the outer wheel is limited in proportion to the excess speed of the outer wheel compared to the non-driving wheel to prevent power slides. (2) Oversteer prevention logic can reduce overshooting yaw motion during severe

lane changes. The algorithm transmits driving torque from the outer wheel to the inner wheel in proportion to the level of excess yaw rate relative to the target yaw rate. (3) A cooperative control strategy with an electronic stability control (ESC) system is developed to decouple the ELSD/ESC system from the overlapped control timing. (4) Steering feel compensation logic is applied to the electric power-assist steering to prevent a torque steer effect caused by torque bias. The performance of the proposed algorithm has been investigated via vehicle tests. The proposed algorithm has been verified through patents on the control method and friction estimation approach for the novelty of this research. The ELSD with the proposed algorithm was then applied to mass production. This approach received positive feedback from international media due to the significant improvements in vehicle performance via ELSD. The system with the proposed algorithm also was won the IR52 Jang Young-shil Award for its technological importance, originality, economic value, and technical spill-over.

Keywords: Electronic Limited Slip Differential (ELSD), Yaw Damping, Tire-road Friction Estimation, Wheel Spin, Friction Circle

Student Number: 2012-30178

List of Figures

Table of Contents

Chapter 1 . Introduction

1.1. Background and Motivation

Front-wheel-drive (FWD) high-performance cars can be developed in combination with high-powered engines based on existing compact or subcompact car platforms. Therefore, high-performance cars can be developed with a relatively low cost. However, it is important for high-performance cars to reflect good handling performance during acceleration in turn as well as accelerating performance.

However, conventional FWD cars have consequential disadvantages including a lack of accelerating performance and excessive understeer—a phenomenon in which the turning radius becomes larger than the driver's intention—during acceleration in turn because slipping of the inner driving wheel upon turning can occur with a small vertical load on the wheel as shown in Figure 1.1.
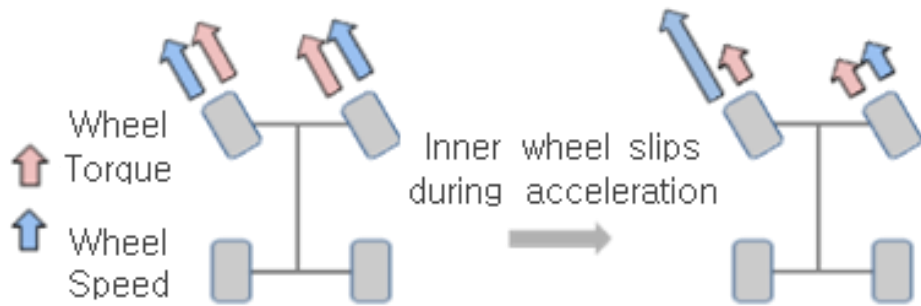
Figure 1.1. Issue of acceleration in turns with open differential.

This understeer can be minimized and acceleration performance can be improved by transferring torque from the inner wheel (which reduces grip) to the outer wheel (which increases grip).

1.2. Previous Researches

A number of studies have been introduced for the development of torque management to compensate the consequential disadvantages, which include lack of acceleration and excessive understeer in FWD high-performance car.

To solve this problem, inner wheel braking control with an electronic stability control (ESC) system has also been used (Uematsu and Gerdes, 2002; Heißing and Metin, 2010) as shown in Figure 1.2.

ESC systems to control inner wheel braking have the advantages of using an existing system. However, there are disadvantages in terms of reducing the overall acceleration force in terms of the amount of applied braking force. In addition, if the brake is applied with a large amount of control command, then it may cause a problem such as disturbing drivers (Chen et al., 2013; Song et al., 2015; Joa et al., 2017). Therefore, either the level of braking control must be limited, or the region where the controller operates must be limited (Lutz et al., 2017). The result is that optimal performance during acceleration in turn cannot be delivered because of the limitations in inner wheel slip control when a large amount of driving torque is applied. It is also necessary to take measures against overheating of the braking system according to an increase in the frequency of brake operation.

Open Differential (OD)	OD + Inner Side Braking	Limited Slip Differential
3000 Nm	3000 Nm	3000 Nm
Engine Torque Truncation		
1000 Nm 1000 Nm	1000 Nm 1500 Nm	1000 Nm 2000 Nm
Curve Inner Curve Outer	Curve Inner -500 Nm Curve Outer	Curve Inner Fixed Ratio Curve Outer
• Engine torque is reduced to deliver 1000 Nm to each wheel	• Engine torque is not reduced. • Wheel brake absorbs 500 Nm to prevent the wheel slipping	• Engine torque is not reduced. • Multiplate clutch packs and gears can transfer the torque asymmetrically

Figure 1.2. Alternative torque vectoring method.

Another method is a mechanical limited slip differential (MLSD). The MLSD applies friction torque to restrict the rotational degrees of freedom about the left and right wheels as shown in Figure 1.3.
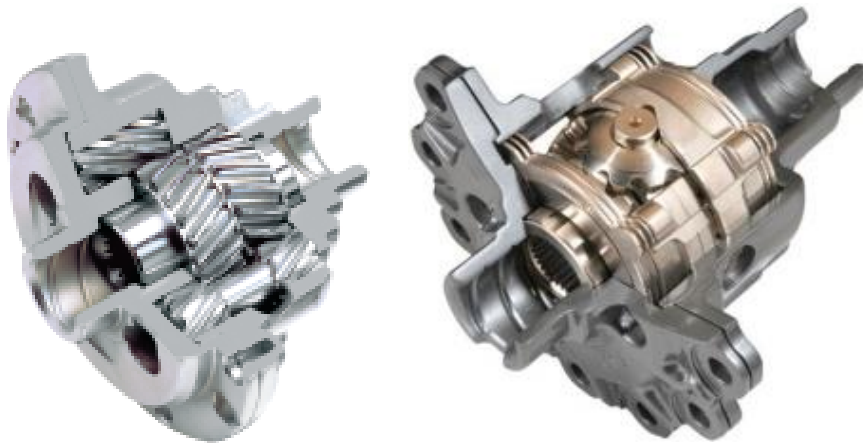
Figure 1.3. MLSD by helical gear or multi-plate (courtesy of GKN).

4

The purpose of a MLSD-related paper was to improve vehicle handling and traction performance (Platteau et al., 1995). Some papers introduced examples about drifting control by rear-wheel-drive (RWD) cars (Velenis et al., 2011; Goh, and Gerdes, 2016; Joa et al., 2020). A paper presented an analytical evaluation of the performance of MLSD (Shan and Bowerman, 2002).

There are two types of method for applying the friction torque: the gear friction method (in which the friction torque is increased by the reaction force acting on the gear) and the multi-plate clutch method (in which the friction torque is increased by reaction force acting on the multi-plate).

The torque of a wheel is reduced when that wheel is spinning without traction due to the fact that the driving torque is transferred from the fast shaft to the slow shaft when the degrees of freedom about the left and right wheels are restricted by the friction torque; thus, the torque can be transferred to the wheel that has traction. The ratio of the torque of the receiving shaft to the torque of the deprived shaft is called the torque bias ratio (TBR).

However, there is no function that can control this differential limiting function (so that it is only applied when needed) as shown in Figure 1.2. Therefore, the TBR cannot be set to a high value because of the many adverse effects that result from a limited differential; rather, it is set by compromising on a suitable value.

The major adverse effect is the case in which the driving force is distributed in the direction that increases understeer and oversteer, which is the opposite of its distribution in the decreasing direction. Furthermore, FWD vehicles may have significant torque steer problems caused by the difference in drive torque between the left and right wheels (Woo et al., 2007). In addition, during a maneuver with a large steering angle that is close to a full turn, vibrations and noise can occur as the tires slip because of the loss of the differential function. This leads to a speed difference between the left and right wheels.

Therefore, the electronic limited slip differential (ELSD) was developed to control the occurrence of friction torque to limit the differential as required. ELSD controls the degree of restriction via an electrical hydraulic multi-disc clutch to restrict the rotational degrees of freedom about the left and right wheels as shown in Figure 1.4.

Figure 1.4. ELSD for RWD car (courtesy of GKN).

Most ELSD-related papers were aimed to improving vehicle stability (Sasaki et al., 1994; Piyabongkarn et al., 2006; Hancock et al., 2007; Piyabongkarn et al., 2007; Damrongrit et al., 2010; Assadian et al., 2010; Mashadi et al., 2011; Rubin and Arogeti, 2015). The purpose of a paper was to improve traction performance on low friction surfaces (Kinsey, 2004). Some papers introduced examples of stability and traction improvements (Piyabongkarn, Lew, Grogg, and Kyle, 2006; Fox and Grogg, 2012). A paper

presented detailed and reduced dynamic models for the simulation of ELSD (Morselli et al., 2006).

Unfortunately, research to improve vehicle agility is lacking. The reason why research on ELSD has been conducted mainly for the purpose of stability and traction performance is that ELSD is mainly installed in RWD high-power cars or SUVs that have a high demand for stability and traction performance.

Basically, ELSD can limit torque transfer from the fast wheel to the slow wheel because torque distribution is achieved by restricting the degrees of freedom about the right and left wheels by friction using a clutch. Therefore, there are limited conditions under which ELSD can create driving torque distributions that control understeer. For example, during normal driving in which the outer wheel turns faster than the inner wheel, understeer reduction control cannot be performed. Moreover, the control intervention point must be determined accurately to reduce understeer.

BorgWarner introduces the world's first ELSD designed for the front transaxle of a FWD high-performance vehicle on the latest Volkswagen Golf (Mk7) GTI with Performance Pack. It was the main competitor when Hyundai's first high-performance car was developed. Of course, the control logic of the competitor's system is not disclosed as a confidential as shown in Figure 1.5.
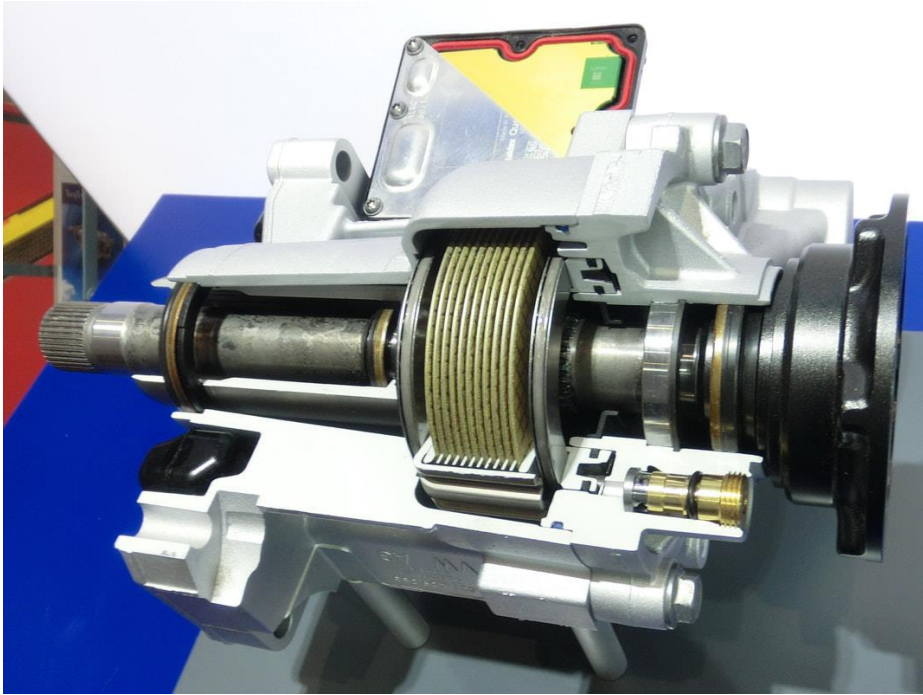
Figure 1.5. World's first ELSD for FWD high-performance car
(courtesy of BorgWarner).

1.3. Thesis Objectives

This dissertation focused on a predictive control strategy for improved handling and acceleration performance of FWD high-performance vehicles with electronic limited slip differential.

For this study, a conceptual analysis with respect to vehicle speed change has been performed on the areas that can be improved via the driving control system as shown in Figure 1.6.

	Vehicle Speed Change			
	Up (Wheel spin)	Up	Maintain	Down

Yaw Moment Direction — Inhibit oversteer / Inhibit understeer

Driving Status	Wheel spin (Inner wheel)	No wheel spin
Wheel Speed	Inner > Outer	Inner < Outer

Legend:
- Demand FWD (red dashed)
- Demand RWD (blue dashed)
- Supply ESC (hatched)
- Supply MLSD (green solid line)
- Supply ELSD (green filled)
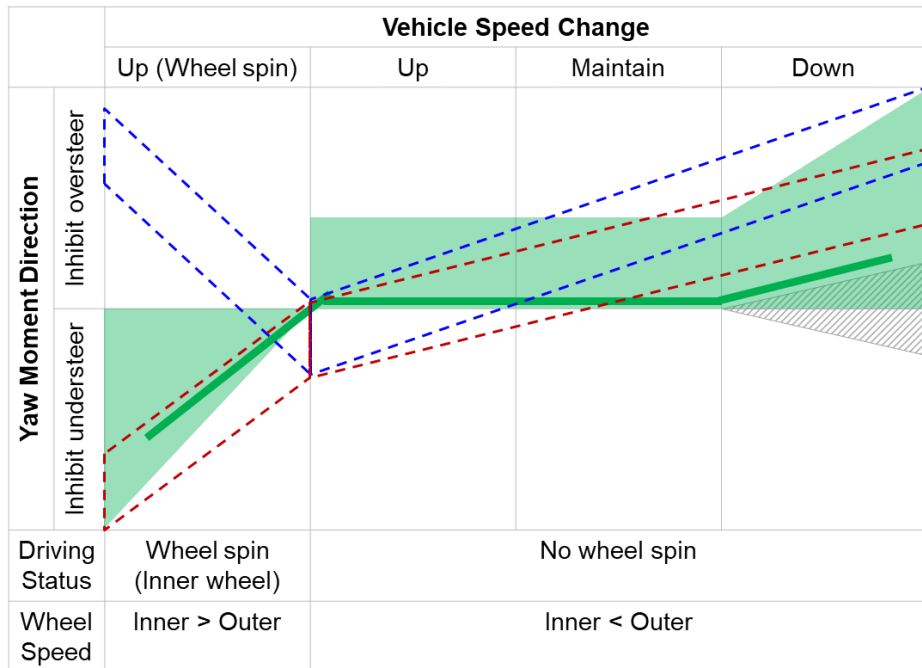
Figure 1.6. A conceptual analysis on the areas that can be improved via the control system according to vehicle speed change.

Figure 1.6 represents supply and demand of yaw moment according to vehicle speed change.

The characteristics of the RWD vehicle are changed in the oversteer direction as it decelerates due to the effect of the load transfer to the front

wheel and the longitudinal force acting on the rear wheel. Therefore, yaw moment control is needed to prevent oversteer. The characteristics of the RWD vehicle are changed in the oversteer direction as it accelerates with wheel spin due to the effect of losing the tire grip of the rear wheel. Therefore, yaw moment control is needed to prevent oversteer.

The characteristics of the FWD vehicle are changed in the oversteer direction as it decelerates due to the effect of the load transfer to the front wheel. Therefore, yaw moment control is needed to prevent oversteer. The characteristics of the FWD vehicle are changed in the understeer direction as it accelerates with wheel spin due to the effect of losing the tire grip of the front wheel. Therefore, yaw moment control is needed to prevent understeer.

ELSD's torque supply can best meet demand of FWD high-performance vehicles. Especially, this dissertation focuses on increasing yaw moment for preventing understeer during acceleration in turns. Meanwhile, the ESC using the braking system must slow down to generate a yaw moment.

Another conceptual analysis with respect to driving wheel speed difference was performed on the areas that can be improved via the driving control system as shown in Figure 1.7
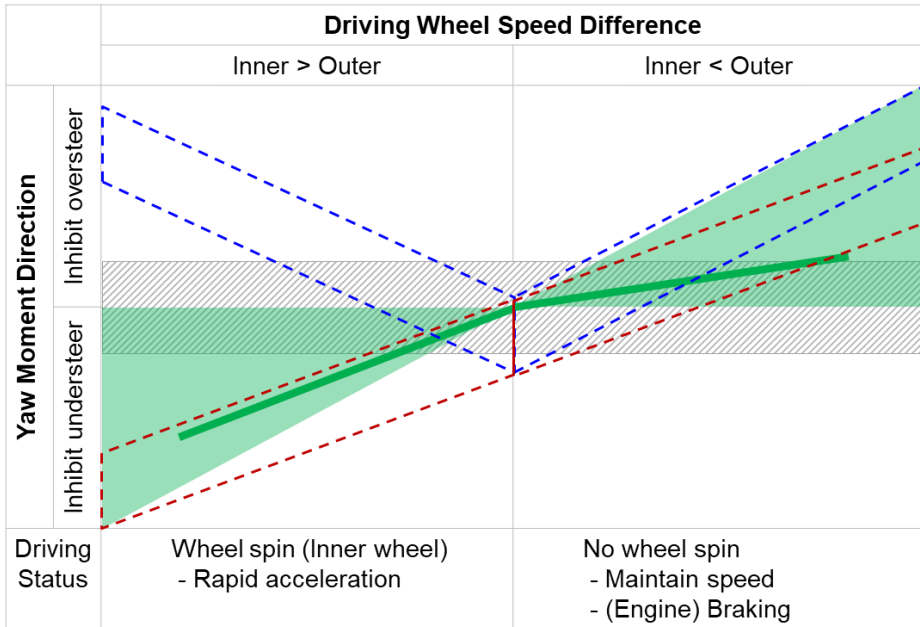
Figure 1.7. A conceptual analysis on the areas that can be improved via the control system according to driving wheel speed difference.

Figure 1.7 represents supply and demand of yaw moment according to driving wheel speed difference.

ELSD's torque supply can best meet demand of FWD high-performance vehicles. However, there is little paper about for increasing yaw moment, because the research on ELSD has been conducted mainly for the purpose of

vehicle stability. The main reason is that ELSD installed in RWD high-power cars or SUVs that have a high demand for stability and traction performance. It is also easy to control for decreasing yaw moment because an operation ELSD prevent yaw motion in normal turning condition, when the inner wheel speed is slower than the outer wheel speed.

This dissertation focused on increasing yaw moment logic to prevent understeer during acceleration in turns for FWD high-performance vehicles. In terms of the characteristic of the system, ELSD has the potential to promote not only handling performance but also accelerating performance. It is possible to increase yaw moment via operation ELSD only when the inner wheel speed becomes greater than the outer wheel speed during a turn. This condition usually occurs when the inner wheels spin.

Therefore, the increasing yow moment in ELSD control has main challenge on determining operation condition when the inner wheel will be faster than the outer wheel, because the inner wheel suddenly becomes faster than the outer wheel after wheel spin. It means that the direction of yaw moment via ELSD is changed from negative to positive abruptly.

Here, an algorithm is proposed to determine the control conditions for accurately decreasing or increasing understeer considering its torque transfer characteristic. In particular, a prediction model about wheel spin is proposed for setting the accurate intervention time to reduce the understeer that occurs during acceleration in turn. This is a function that is needed mainly for FWD high-performance vehicles. Considering operation delay of the ELSD, the prediction model estimates allowable driving force to predict wheel spin, due

14

to the fact that the driving force is a leading factor relative to the wheel speed.

1.4. Thesis Outline

This dissertation is structured in the following manner. An Analysis of lateral torque transfer of ELSD system is described in Chapter 2. In Chapter 3, ELSD handling control algorithm overview is introduced. In Chapter 4, control logic for understeer prevention is introduced and describes the simple models for predictive control of wheel spin. In Chapter 5, Control logic for oversteer prevention is introduced. Then an algorithm for yaw rate feedback control is designed based on target yaw rate estimation. In Chapter 6, control strategy for other control systems is introduced. In Chapter 7, Tire-road friction estimation to improve the predictive control is introduced. Chapter 8 shows the test results for the evaluation of the performance of the proposed ELSD control algorithm. Then the conclusion which describes the summary and contribution of the proposed ELSD control algorithm and future works is presented in Chapter 9.

Chapter 2 . Analysis of Lateral Torque Transfer of Electronic Limited Slip Differential (ELSD) System

One of the most efficient methods for controlling the left–right distribution of the driving force is to add a clutch to the existing differential gear as shown in Figure 2.1.
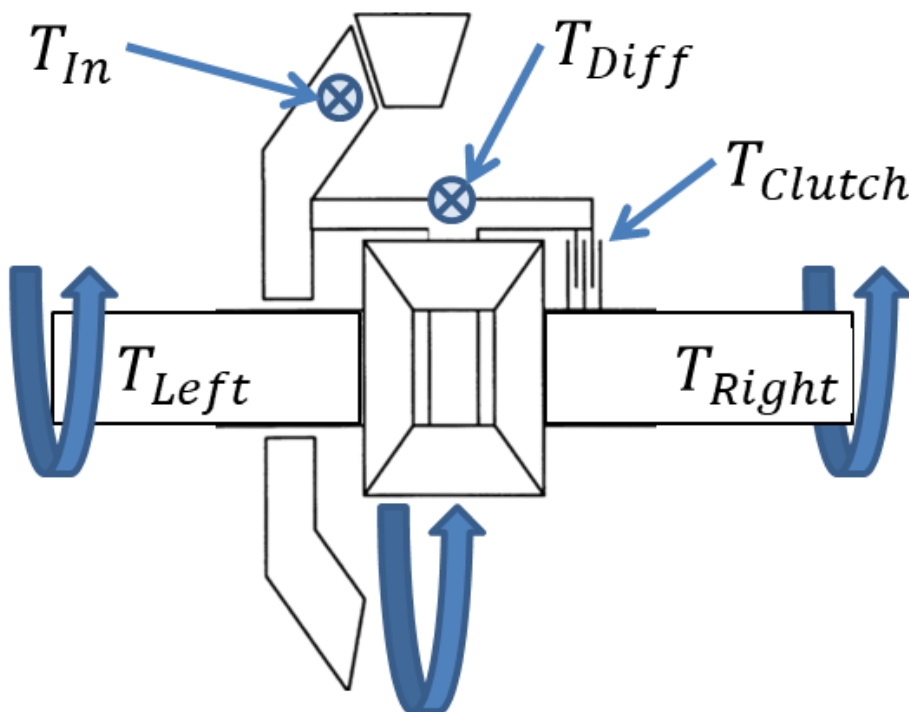
Figure 2.1. Schematic of ELSD.

Where T_{In} denotes the input torque from transmission, T_{Diff} denotes the torque transferred by differential gear, T_{Clutch} denotes the torque transferred by clutch, T_{Left} denotes the output torque to left drive shaft, T_{Right} denotes the output torque to right drive shaft. $\otimes$ denotes the tangential direction of the forward rotation.

  Then an additional driving force transfer path is created between one of the side gears and the ring gear. Therefore, the left–right wheel driving distribution can be controlled by adjusting the clutch's degree of friction as shown in the equations below.

$$T_{In} = T_{Diff} + T_{Clutch} \tag{2.1}$$

$$T_{Left} = \frac{T_{Diff}}{2} \tag{2.2}$$

$$T_{Right} = \frac{T_{Diff}}{2} + T_{Clutch} \tag{2.3}$$

If Eq. (2.1) and (2.2) are combined, and Eq. (2.1) and (2.3) are combined,

$$T_{Left} = \frac{T_{in} - T_{Clutch}}{2} \tag{2.4}$$

$$T_{Right} = \frac{T_{in} + T_{Clutch}}{2} \tag{2.5}$$

Assumptions:

  - The moment of inertia of each driving part is ignored.

  - The loss from each driving part is ignored.

    An ELSD uses an electronically controlled clutch to restrict the left–right rotational degrees of freedom about the differential gear and to synchronize the left and right wheel speeds. Therefore, the driving torque can be transferred from the fast wheel to the slow wheel as shown in Figure 2.2.
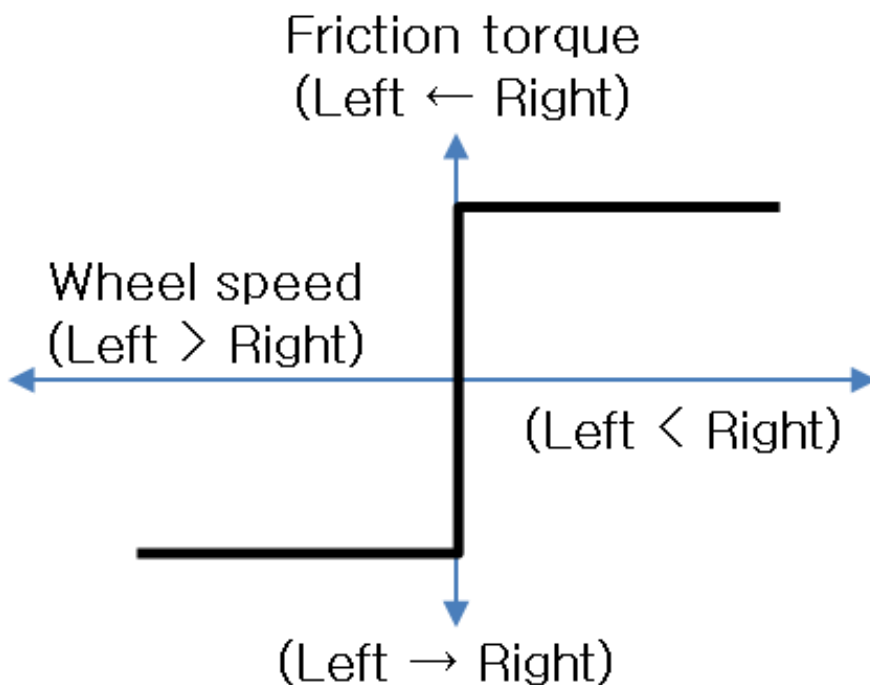
Figure 2.2. Torque transfer characteristic of clutch.

The x-axis represents speed difference of driving wheel, right wheel minus left wheel. Figure 2.2 represents torque transfer by the friction of the clutch with respect to speed difference of driving wheel.

Figure 2.3 shows that more driving torque is transferred from the inner wheel to the outer wheel as the ELSD power increases when the inner wheel speed becomes greater than the outer wheel speed during a turn. Thus, it is possible to control the steering in a direction that reduces understeer. In other situations where the inner wheel speed is less than the outer wheel speed, more driving torque is transferred from the outer wheel to the inner wheel as the ELSD power increases. It is more likely to control the vehicle in a direction that reduces oversteer.
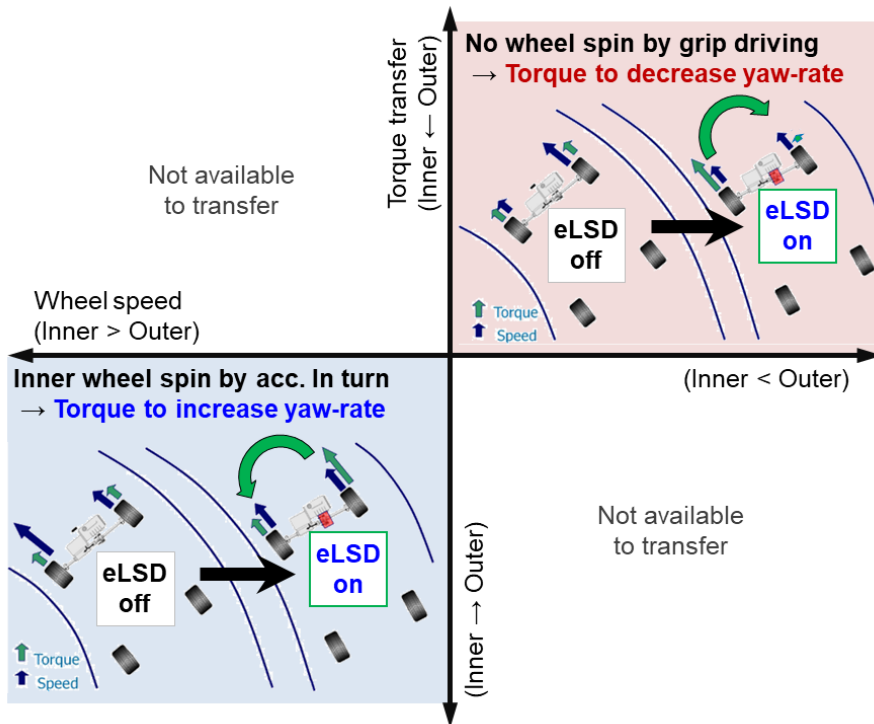
Figure 2.3. Areas and conditions for ELSD control is activated.

The x-axis represents speed difference of driving wheel, outer wheel minus inner wheel. The y-axis represents torque transfer by the ELSD.

Chapter 3 . Electronic Limited Slip Differential (ELSD) Handling Control Algorithm Overview

In general, understeer prevention control should performed when the vehicle's actual yaw rate is less than the target yaw rate and oversteer prevention control is needed when the vehicle's actual yaw rate is greater than the target yaw rate to improve handling performance as shown Figure 3.1 and the following equations.
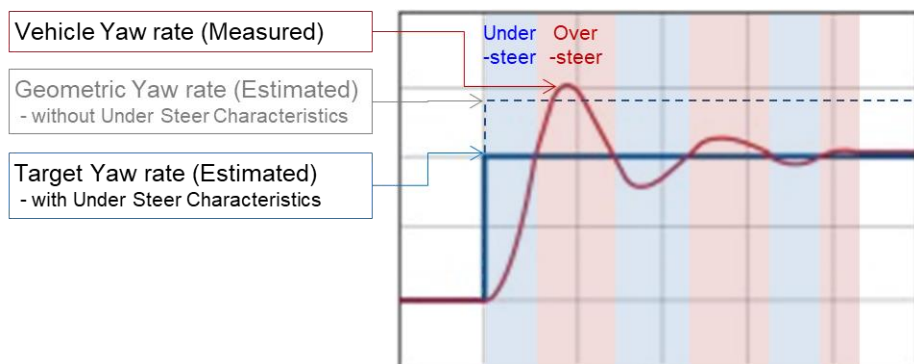
Figure 3.1. General handling control strategy.

Figure 3.1 represents yaw rate with respect to time.

$$\dot{\Psi}_{Geometry} = \frac{v}{L+v^2} \cdot \delta \tag{3.1}$$

$$\dot{\Psi}_{Target} = \frac{v}{L+K_{US} \cdot v^2} \cdot \delta = \frac{v}{L+(L/v_{ch}) \cdot v^2} \cdot \delta \tag{3.2}$$

Where $\dot{\Psi}_{Geometry}$ denotes the geometric yaw rate without understeer characteristic of a vehicle, $\dot{\Psi}_{Target}$ denotes the target yaw rate with understeer characteristic, v denotes the vehicle speed, L denotes the wheel base, K_{US} denotes the understeer gradient, δ denotes steer angle of road wheel, v_{ch} denotes the characteristic speed.

Considering the torque transfer mechanism of ELSD clutch as presented in chapter 2, the ELSD handling control strategy is as shown in Figure 3.2 and the following equations.
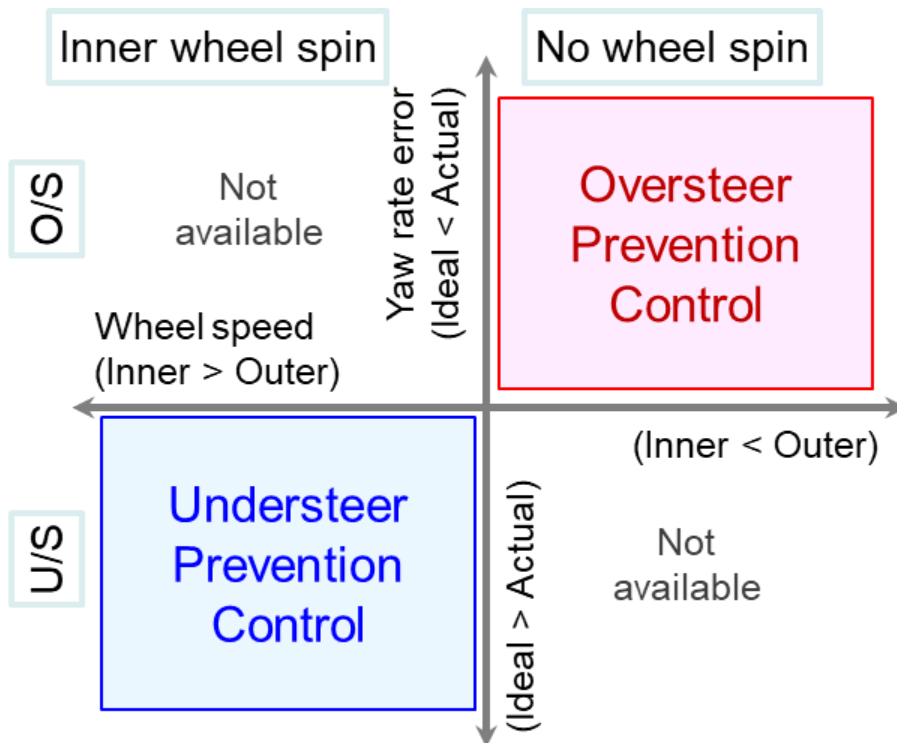
Figure 3.2. ELSD handling control strategy.

The x-axis represents speed difference of driving wheel, outer wheel minus inner wheel. The y-axis represents yaw rate error, actual sensing value minus Ideal estimated value. Understeer prevention control is performed when the vehicle's actual yaw rate is less than the target yaw rate, and the inner wheel speed is greater than the outer wheel speed. Oversteer prevention control occurs when the vehicle's actual yaw rate is greater than the target yaw rate, and the inner wheel speed is less than the outer wheel speed.

One characteristic of the ELSD is that it is activated when a wheel slip

difference occurs during driving, and driving torque is transferred to the wheel that still has enough road friction to support additional driving force. This leads to a smooth and straight exit from split-mu road surface.

In addition to the handling control, ELSD also includes straight-acceleration control logic for exits on roads where tire grip is lost by one wheel either on the left or right side. The ELSD logic is configured as shown in Figure 3.3 and the following equations.
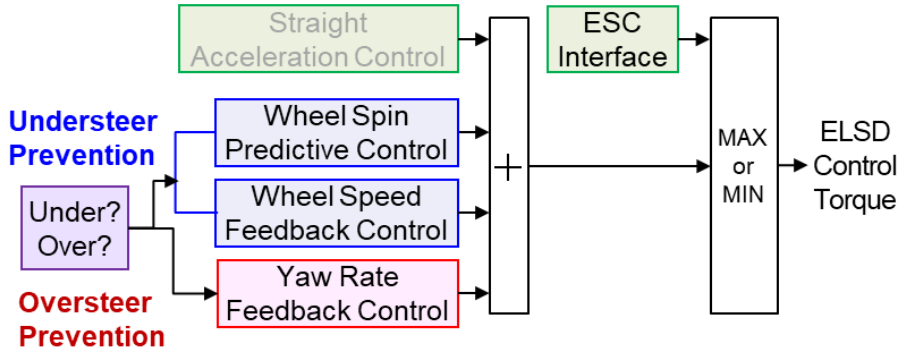
Figure 3.3. ELSD logic outline.

$$T_{ELSD} = T_{ELSD\_WSP} + T_{ELSD\_WSF} + T_{ELSD\_YRF} + T_{ELSD\_SA} \tag{3.3}$$

Understeer prevention control ($T_{ELSD\_WSP}, T_{ELSD\_WSF}$) is activate when

$$\left[\left(\Psi_{Real} - \Psi_{Target}\right) < \Psi_{Under\_on}\right] \& \left[\left(\omega_{in} - \omega_{out}\right) \geq \omega_{Under\_on}\right] \tag{3.4}$$

Understeer prevention control ($T_{ELSD\_WSP}, T_{ELSD\_WSF}$) is Deactivate when

$$[(\dot{\Psi}_{Real} - \dot{\Psi}_{Target}) \geq \dot{\Psi}_{Under\_off}] \,\&\, [(\omega_{in} - \omega_{out}) < \omega_{Under\_off}] \qquad (3.5)$$

Oversteer prevention control (T_{ELSD_YRF}) is activate when

$$[(\dot{\Psi}_{Real} - \dot{\Psi}_{Target}) \geq \dot{\Psi}_{Over\_on}] \,\&\, [(\omega_{in} - \omega_{out}) < \omega_{Over\_on}] \qquad (3.6)$$

Oversteer prevention control (T_{ELSD_YRF}) is Deactivate when

$$[(\dot{\Psi}_{Real} - \dot{\Psi}_{Target}) < \dot{\Psi}_{Over\_off}] \,\&\, [(\omega_{in} - \omega_{out}) \geq \omega_{Over\_off}] \qquad (3.7)$$

Where T_{ELSD} denotes the total ELSD control torque, T_{ELSD_WSP} denotes the ELSD control torque by wheel spin predictive control, T_{ELSD_WSF} denotes the ELSD control torque by wheel speed feedback control, T_{ELSD_YRF} denotes the ELSD control torque by yaw rate feedback control, T_{ELSD_SA} denotes the ELSD control torque by straight acceleration control which is not included in this research, $\dot{\Psi}_{Real}$ denotes the real yaw rate from sensor, ω_{in} denotes the inner wheel angular velocity, ω_{out} denotes the outer wheel angular velocity, $\dot{\Psi}_{Under\_on}$ denotes the yaw rate offset to activate understeer prevention control, ω_{Under_on} denotes the wheel speed offset to activate understeer prevention control, $\dot{\Psi}_{Under\_off}$ denotes the yaw rate offset to deactivate understeer prevention control, ω_{Under_off} denotes the wheel speed offset to deactivate understeer prevention control, $\dot{\Psi}_{Over\_on}$ denotes the yaw rate offset to activate oversteer prevention control, ω_{Over_on} denotes the wheel speed offset to activate oversteer prevention control, $\dot{\Psi}_{Over\_off}$ denotes the yaw rate offset to deactivate oversteer prevention control, ω_{Over_off} denotes the wheel speed offset to deactivate oversteer prevention

control.

Chapter 4 .   Control   Logic   for Understeer Prevention

Understeer prevention logic is developed for acceleration in turn. First, for a rapid response, the driving torque is transferred in advance from the inner to the outer wheels considering the magnitude of the estimated traction potential in the wheels. If wheel spin occurs due to estimation error, then additional driving torque is transmitted according to the wheel speed status of the inner wheel, the outer wheel, and reference wheel (non-driving wheel) as shown in Figure 4.1.
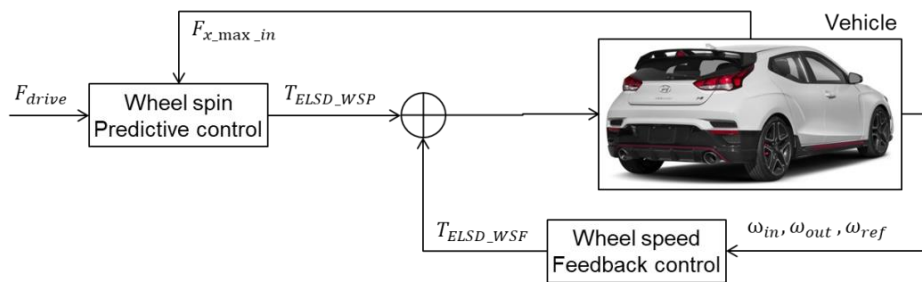
Figure 4.1. Control logic diagram for understeer prevention.

4.1. Wheel Spin Predictive Control

4.1.1. Model-based Predictive Control Overview

The inner wheels of front-wheel-driving vehicles spin when a driving torque greater than the inner wheel grip is applied because of an increase in pressure on the accelerator pedal during acceleration in turn. This spinning results in understeer, and the reduction of exit acceleration. Therefore, these can be overcome by controlling the inner wheel slip via electronic limited slip differential (ELSD) when the inner wheel speed becomes greater than the outer wheel speed via inner wheel spin during an accelerated exit as shown in Figure 4.2.
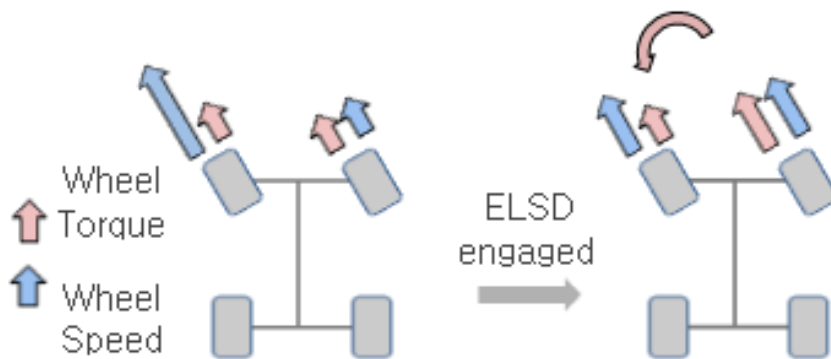
Figure 4.2. Wheel spin & understeer reduction when ELSD is operated.

However, if control is performed after wheel slip is observed, then the initial wheel spin cannot be controlled properly because of the time delay in

the operation of the system as shown in Figure 4.3.
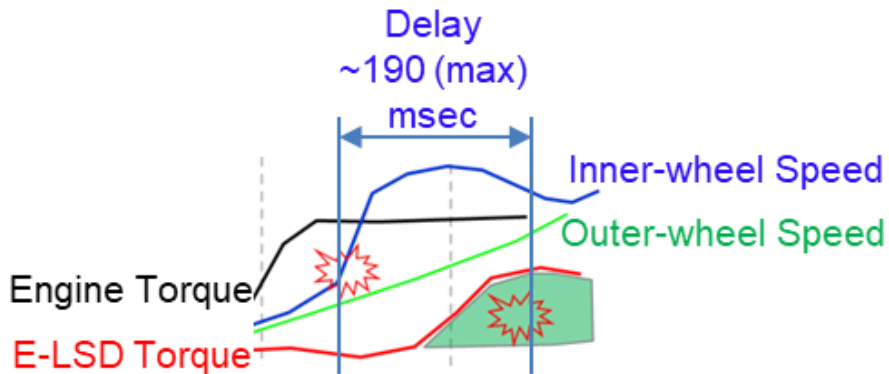
Figure 4.3. The concept of ELSD intervention time delay.

Figure 4.3 represents engine torque, wheel speed, and ELSD engaging torque, respectively with respect to time. The driving torque from the engine is presented in a black line. The inner-wheel speed is illustrated in a blue line. A green line is outer-wheel speed. A red line presents the engaging torque of ELSD.

The time delay consists of two parts. One is slew rate via ELSD actuator, the other is Zero-order hold by sampling time of controller. The maximum delay by the actuator is 180msec to ramp up to maximum torque). And the sampling time of the control logic is 10msec. Therefore, maximum total time delay is up to 190msec, and intermediate total time delay is by 95msec as shown in Figure 4.4.
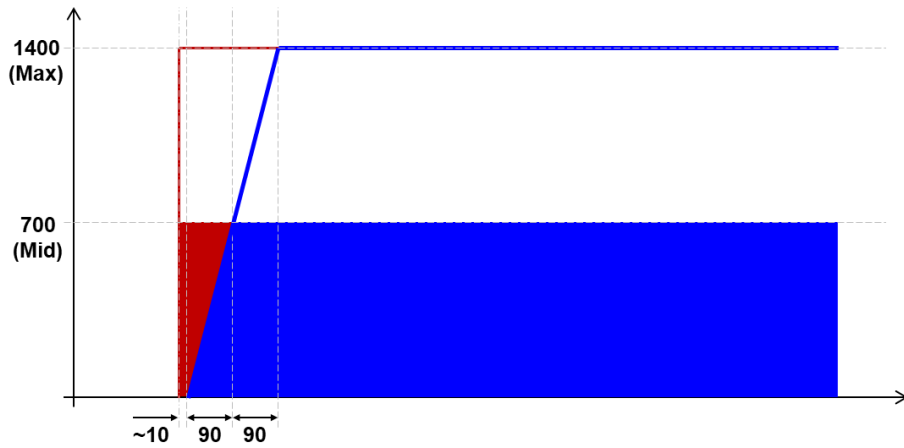
Figure 4.4. Delay characteristic of ELSD with proposed logic.

Figure 4.4 represents ELSD engaging torque with respect to time.

However, if the ELSD intervention time is moved too far forward to prevent this problem and the differential gear is locked when the outer wheel is faster, then a reverse effect that increases understeer occurs as shown in Figure 4.5. Thus, there is a need for a controller that can predict inner wheel slipping in advance and perform suitable preemptive control.
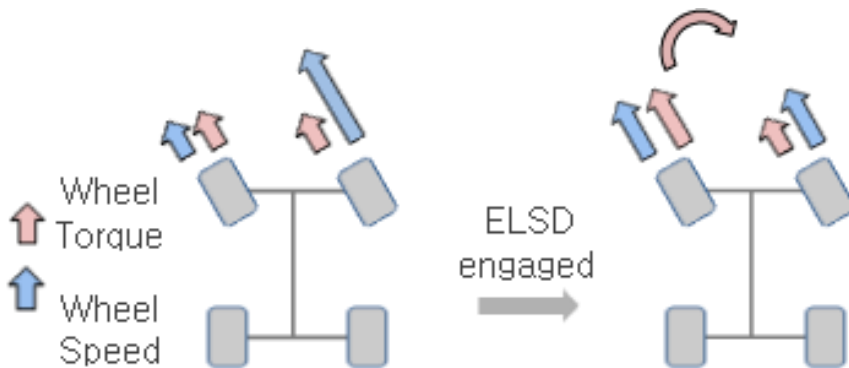
Figure 4.5. Increase in understeer due to early operation of ELSD.

4.1.2. Allowable Driving Force Prediction Modeling

A control algorithm was created to predict inner wheel spinning during acceleration in turn and calculate the friction limit at which the inner wheel can be driven in real time. The results are used to transfer the driving force acting on the inner wheel to the outer wheel by the amount that exceeds the calculated limit. In the model that calculates the inner wheel's friction limit in real time, the lateral acceleration sensor signal value is used as the input to calculate the load transfer through which the vertical load of the inner wheel can be estimated in turn as shown in Figure 4.6. The inner wheel's friction limit is then calculated as the product of the friction coefficient of the road surface and the inner wheel vertical load.
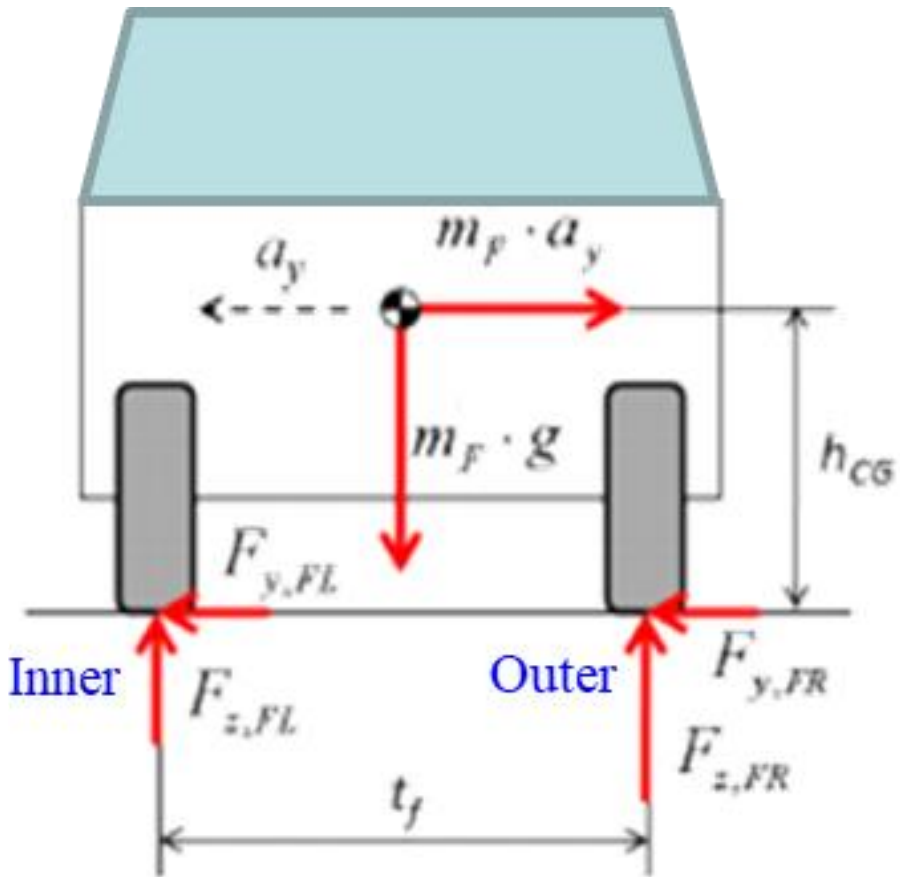
Figure 4.6. Load transfer model that uses lateral acceleration.

However, according to the tire friction circle concept, the driving force limit can be reduced through the extent of the lateral force even about the same resulting friction limit. Therefore, an allowable driving force prediction model was created according to the lateral force as shown in Figure 4.7 with the following equations.
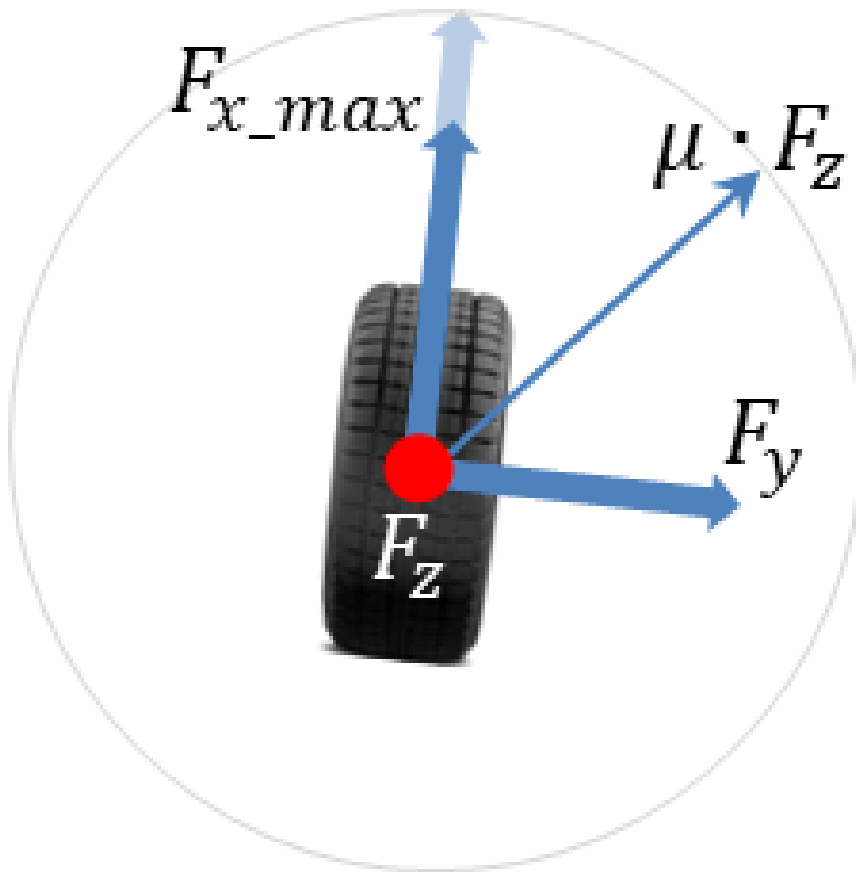
Figure 4.7. Driving force limitation according to acting lateral force.

$$F_{x\_max}^2 + F_y^2 = (\mu \cdot F_z)^2 \tag{4.1}$$

$$F_{x\_max} = \sqrt{\mu^2 - (\frac{a_y}{g})^2} \cdot F_z \tag{4.2}$$

Where F_{x_max} denotes the allowable tire driving force, F_y denotes the tire

lateral force, μ denotes the friction coefficient, F_z denotes the tire vertical force, a_y denotes the lateral acceleration, g denotes the gravity acceleration.

Hence, the logic is designed for the ELSD clutch to be engaged in proportion to the amount that the real driving force from the powertrain exceeds the allowable driving force at inner wheel. Therefore, ELSD is activated when the engaging value is greater than 0, which means that inner wheel spin occurs because the driving force of the engine is greater than the allowable driving force as shown in Figure 4.8 with the following equations.
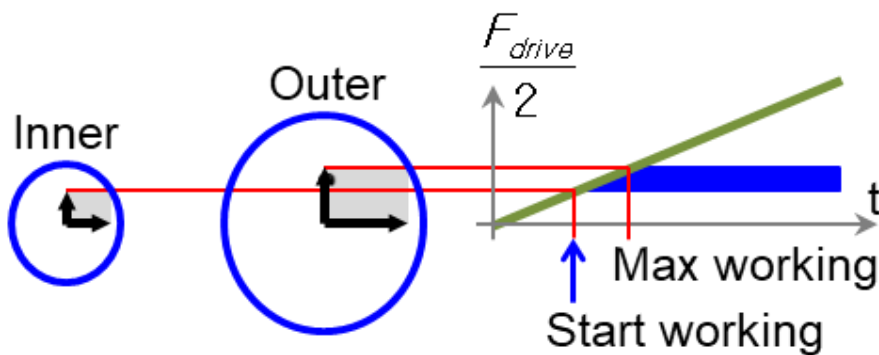
Figure 4.8. The concept of ELSD operation time and control amount.

Figure 4.8 represents the driving force expected to be applied to each wheel with respect to time.

$$\frac{F_{Drive}}{2} = \frac{T_{drive} - I_{drive} \cdot \ddot{\theta}_{drive}}{2 \cdot R_{tire}} \tag{4.3}$$

$$T_{ELSD\_WSP} = 2 \cdot \left(\frac{F_{drive}}{2} - F_{x\_\max\_in} \right) \cdot R_{tire} \qquad (4.4)$$

$$T_{ELSD\_WSP} < \left(F_{x\_\max\_out} - F_{x\_\max\_in} \right) \cdot R_{tire} \qquad (4.5)$$

Activate when

$$\left(\frac{F_{drive}}{2} - F_{x\_\max\_in} \right) \geq F_{On} \qquad (4.6)$$

Deactivate when

$$\left(\frac{F_{drive}}{2} - F_{x\_\max\_in} \right) < F_{Off} \qquad (4.7)$$

Where T_{ELSD_WSP} denotes the ELSD control torque by wheel spin predictive control, $\frac{F_{drive}}{2}$ denotes the driving force from powertrain to each wheel, $\frac{T_{drive}}{2}$ denotes the driving torque from powertrain to each wheel, I_{drive} denotes the rotational inertia of driveline, $\ddot{\theta}_{drive}$ denotes the rotational acceleration of driveline, R_{tire} denotes the tire radius, $F_{x\_max\_in}$ denotes the inner wheel's traction limit, $F_{x\_max\_out}$ denotes the outer wheel's traction limit, F_{On} denotes the driving force offset to activate predictive control, F_{Off} denotes the driving force offset to deactivate predictive control.

To calibrate the prediction model, two gains are applied. One is to scale the model output, the allowable driving force prediction the other is to scale one of the model input, the signal from lateral acceleration sensor as shown in the

following equation.

$$F_{x\_max} = \text{gain}_{F_x}\sqrt{\mu^2 - (\text{gain}_{F_y} \cdot \frac{a_y}{2})^2} \cdot F_z \qquad (4.8)$$

Where gain_{F_x} denotes the calibration factor to scale the allowable driving force, gain_{F_y} denotes the calibration factor to scale the average lateral force at each tire. As a result, these two calibration factor realize the effect of adjusting the size of the calculated friction circle for each direction as shown in Figure 4.9.
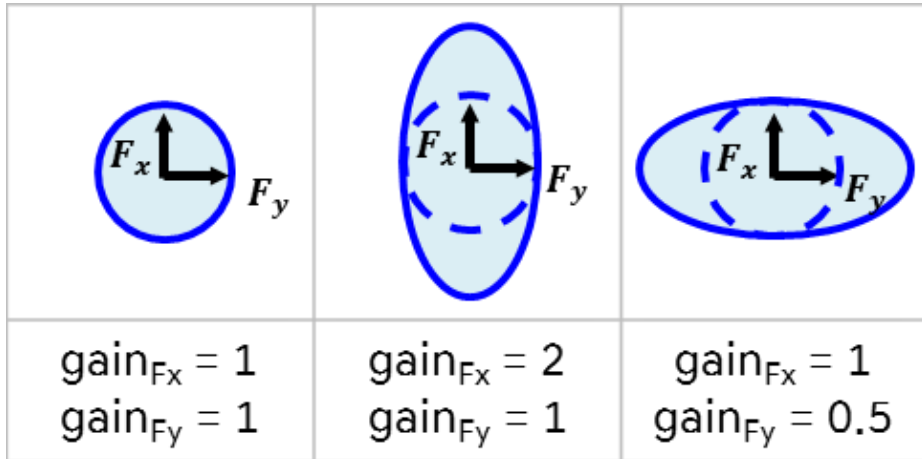
Figure 4.9. The concept of the allowable driving force changes by two gains.

Figure 4.9 represents the longitudinal force of friction circle at each wheel with respect to the lateral force.

4.2. Wheel Speed Feedback Control

If the wheel spin occurs, even with the wheel spin predictive control, the wheel speed feedback control is activated. The wheel speed feedback control consists of two parts, control for inner wheel spin prevention, control for outer wheel spin prevention as shown in the following equation.

$$T_{ELSD\_WSF} = T_{ELSD\_WSF\_in} + T_{ELSD\_WSF\_out} \qquad (4.9)$$

Where T_{ELSD_WSF} denotes the ELSD control torque by wheel speed feedback control, $T_{ELSD\_WSF\_in}$ denotes the ELSD control torque by wheel speed feedback control to prevent inner wheel spin, $T_{ELSD\_WSF\_out}$ denotes the ELSD control torque by wheel speed feedback control to prevent outer wheel spin.

4.2.1. Control for Inner Wheel Spin Prevention

The inner wheel spin prevention control investigates the speed difference between the inner and outer wheels during inner wheel slip. The logic controls the engaging torque of the ELSD clutch linearly according to the speed difference as shown in the following equation and Figure 4.10.

$$T_{ELSD\_WSF\_in} = gain_{WSF\_in} \cdot (\omega_{in} - \omega_{out} - offest_{WSF\_in}) \qquad (4.10)$$

Where $gain_{WSF\_in}$ denotes control gain to calibrate inner wheel speed feedback logic, ω_{in} denotes the inner wheel angular velocity, ω_{out} denotes the outer wheel angular velocity, $offest_{WSF\_in}$ denotes wheel speed offset to calibrate inner wheel speed feedback logic.

Figure 4.10. Control signal for inner wheel spin prevention.

Figure 4.10 represents steering wheel angle, accelerator position, revolution per minute, and operation signal of ELSD with respect to time. The steering wheel angle (SWA) is presented in a red line. The accelerator position (AP) is illustrated in a black line. An orange line is the revolution per minute (RPM). The operation signals of ELSD are represented using 3 lines. The signal of wheel spin predictive control (WSPC) is presented in a dark blue line. The

39

signal of wheel speed feedback control (WSFC)-inner is illustrated in a brown line. A yellow line is the total signal.

Consequently, inner wheel slip control prevents additional wheel slip in cases where wheel slip control via the wheel spin predictive control logic alone is inadequate.

4.2.2. Control for Outer Wheel Spin Prevention

The driving torque can be transferred to the outer wheel by the operation of the ELSD according to the wheel spin predictive control logic or the control logic for inner wheel slip prevention. In this scenario, even the outer turning wheel loses traction when an excessive driving torque is transferred.

In such cases, a sudden understeer occurs as a result of the loss of the outer wheel grip. Thus, the speed of the outer wheel is compared to that of the rear wheels; if the speed difference is found to be excessive, then the ELSD clutch engaging torque is reduced to decrease the sudden understeer as shown in the following equation and Figure 4.11.

$$T_{ELSD\_WSF\_out} = -gain_{WSF\_out} \cdot (\omega_{out} - \omega_{ref} - offest_{WSF\_out}) \qquad (4.11)$$

Where ω_{ref} denotes the reference wheel angular velocity (non-driving wheel), $gain_{WSF\_out}$ denotes control gain to calibrate outer wheel speed feedback logic, $offest_{WSF\_out}$ denotes wheel speed offset to calibrate outer wheel speed feedback logic.
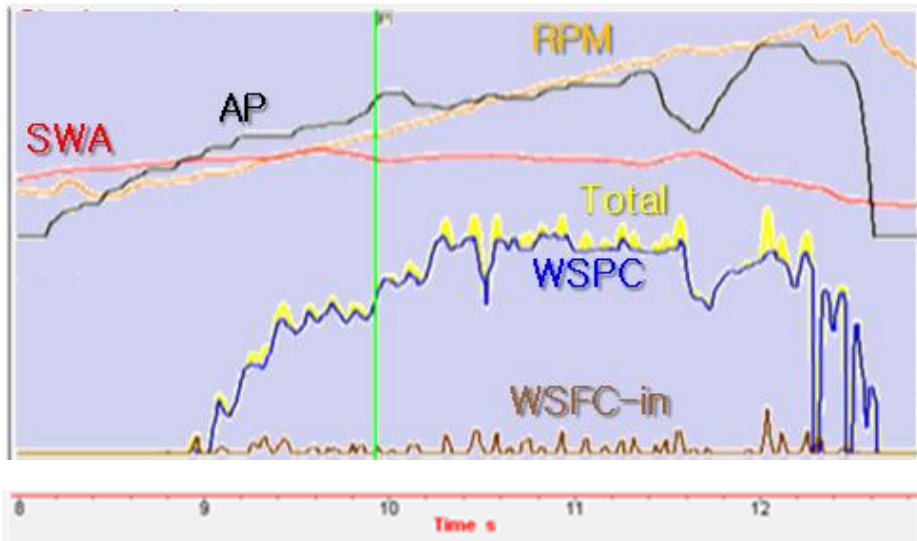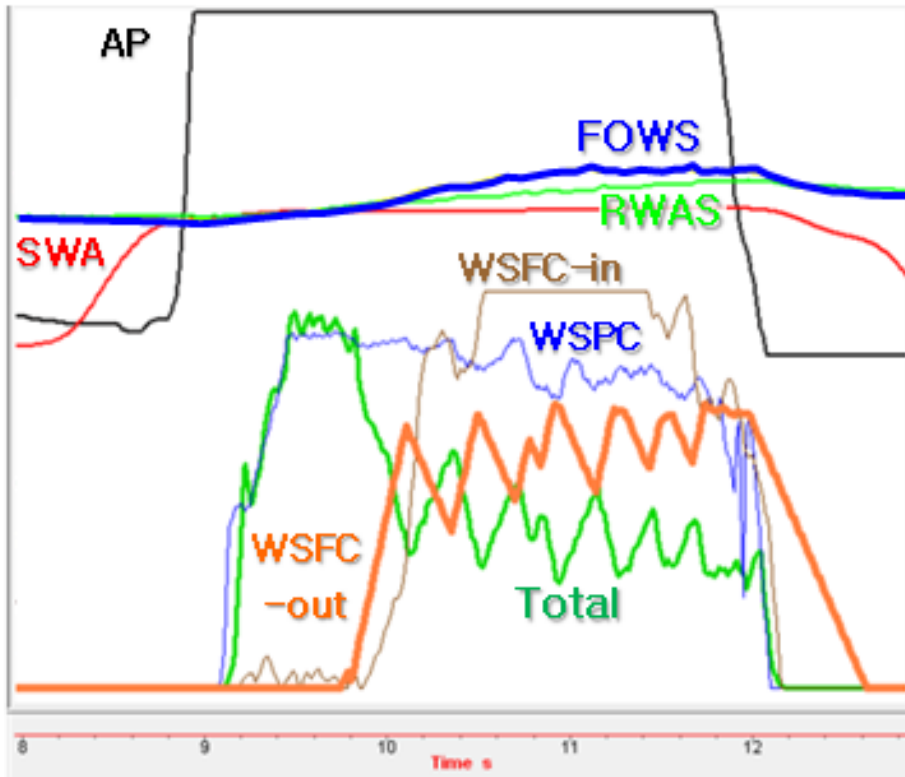
Figure 4.11. Control signal for outer wheel spin prevention.

Figure 4.11 represents steering wheel angle, accelerator position, wheel speed, and operation signal of ELSD with respect to time. The steering wheel angle (SWA) is presented in a red line. The accelerator position (AP) is illustrated in a black line. A blue line is the front outer wheel speed (FOWS). A green line presents the rear wheel average speed (RWAS). The operation signals of ELSD are represented using 4 lines. The signal of wheel spin predictive control (WSPC) is presented in a blue line. The signal of wheel speed

feedback control-inner (WSFC-in) is illustrated in a brown line. An orange line is the signal of wheel speed feedback control-outer (WSFC-out). A green line presents the total signal.

Consequently, outer wheel slip control also prevents additional wheel slip in cases where wheel slip control via the wheel spin predictive control logic alone is inadequate.

4.3. US Prevention Control General Summary

The understeer prevention control strategies are configured through the summarization in Figure 4.12. It shows the operational circumstances of each logic operation during acceleration in turn by an actual scenario. On situation ① when the driving force from engine is greater than the inner wheel driving force limit, the wheel spin predictive control is activated. If situation ② occurs, in which inner wheel slip occurs even with that control, the wheel speed feedback control is activated.
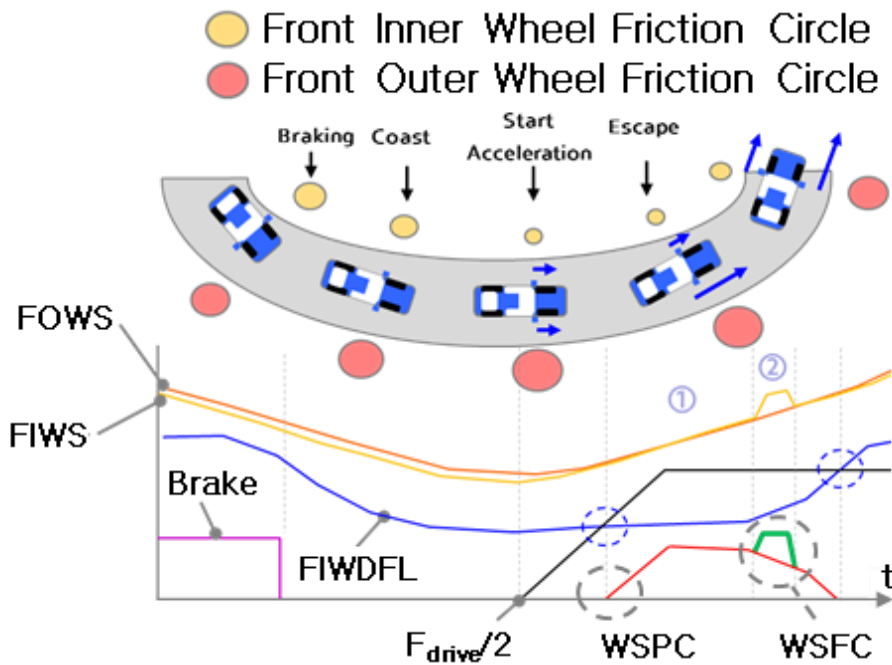
Figure 4.12. The concept of understeer prevention control logic operation.

Figure 4.12 represents brake pedal position, accelerator position, driving force, wheel speed, and operation signal of ELSD with respect to time. The brake pedal position is presented in a magenta line. The driving force is illustrated in a black line. A blue line is the front inner wheel driving force limit (FIWDFL). An orange line presents the front outer wheel speed (FOWS). The front inner wheel speed (FIWS) is presented in a yellow line. The operation signals of ELSD are represented using 2 lines. The signal of wheel spin predictive control (WSPC) is presented in a red line. The signal of wheel speed feedback control (WSFC) is illustrated in a green line.

Considering operation delay of the ELSD, the prediction model estimates allowable driving force to predict wheel spin, because the driving force is a leading factor relative to the wheel speed. However,

It is necessary to review the operation response performance according to the prediction error because predictive control logic is applied to overcome the ELSD operation delay. Basically, driving force is a leading factor relative to the wheel speed. Therefore, the estimated operating point based on the driving force is about 150~200 msec ahead of the determined operating point based on the speed of the wheel as shown as shown in Figure 4.13 with the following equations.
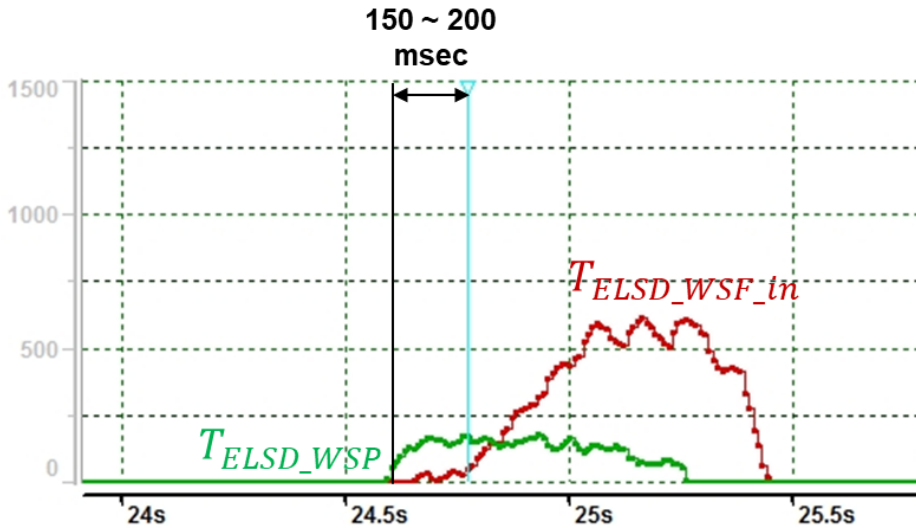
Figure 4.13. Response of force-based control & wheel speed-based control

: The control signal is analyzed itself without operation of ELSD

Figure 4.13 represents ELSD engaging torque with respect to time.

$$T_{ELSD\_WSP} = 2 \cdot \left(\frac{F_{drive}}{2} - \boldsymbol{F_{x\_max\_in}} \right) \cdot R_{tire} \tag{4.12}$$

$$T_{ELSD\_WSF\_in} = gain_{WSF\_in} \cdot \left(\boldsymbol{\omega_{in}} - \boldsymbol{\omega_{out}} - offest_{WSF\_in} \right) \tag{4.13}$$

Considering this difference in operating time, the concept analysis for prediction logic performance via calculation error can be reviewed as shown in Figure 4.14. Even if there is a prediction error, using prediction control logic can improve operational response rather than not using it.

45
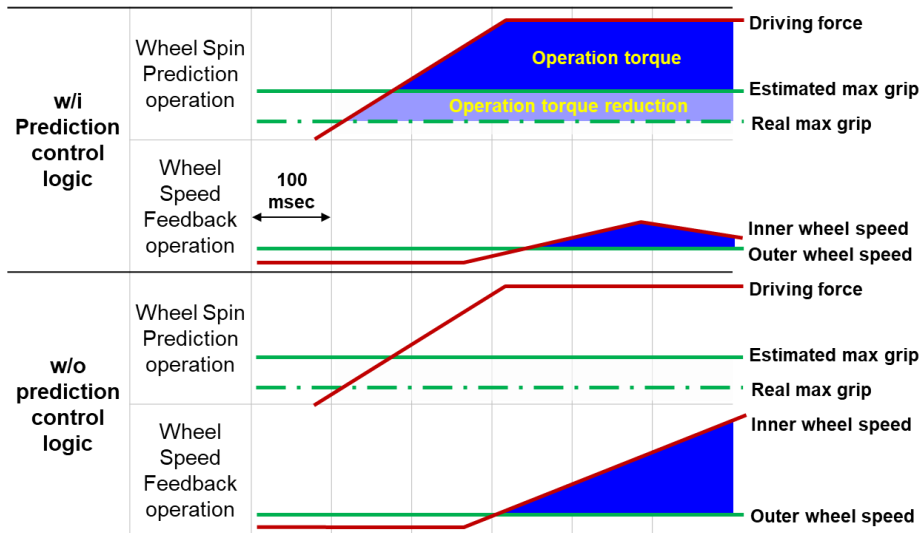
Figure 4.14. Concept analysis for prediction logic performance via calculation error.

Figure 4.14 represents ELSD engaging torque with respect to time.

The wheel torque from actual ELSD operation during corner exit was examined by a wheel force transducer as shown in Figure 4.15. When there was no ELSD, the left and right driving torque values were identical, in other words, the overall both sides of driving torque was limited by the inner wheel slip. However, when the ELSD was activated, the driving torque was transferred from the inner wheel to the outer wheel, and the ratio exceeded 1:3. This is higher than the torque bias ratio (TBR) level of the previously mentioned helical-gear-type mechanical limited slip differential (MLSD),

which is an MLSD that has fewer side effects relatively. It means that a more effective operation can be achieved than MLSD.
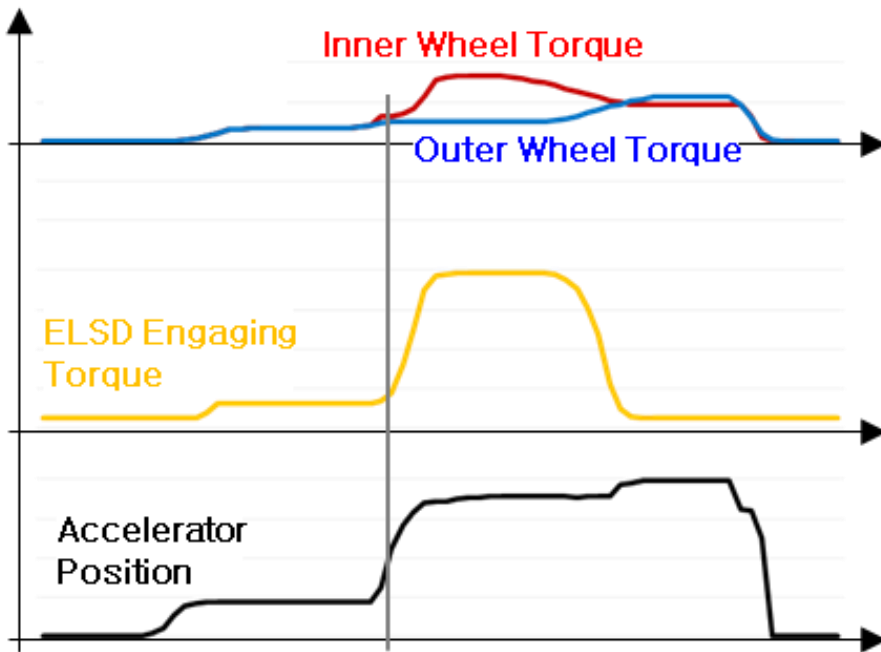
Figure 4.15. Turning inner-outer driving torque when ELSD is activated.

Figure 4.15 represents accelerator position, ELSD engaging torque, and wheel torque with respect to time. The accelerator position is presented in a black line. The ELSD engaging torque is illustrated in a yellow line. A blue line is the front outer wheel speed. A red line presents the front inner wheel speed.

Further, because ELSD allows for unlimited TBR, the TBR measurement value would increase not only when the engine power is increased but also

when the difference between left and right friction circle is increased as shown in Figure 4.16
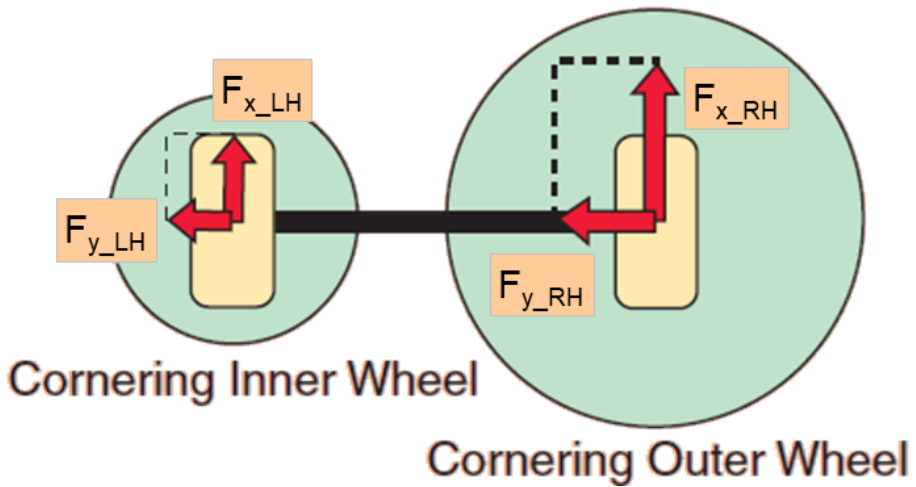
Figure 4.16. TBR via Friction circle difference.

The TBR can be set to a high value by increasing front roll stiffness or by increasing front roll center height as shown in the following equation and Figure 4.17.

$$TBR = \frac{F_{x\_FR}}{F_{x\_FL}} \tag{4.11}$$

$$= \frac{Friction\_circle_{\_FR}}{Friction\_circle_{\_FL}} \tag{4.12}$$

$$= \frac{F_{z\_FR}}{F_{z\_FL}} \tag{4.13}$$

$$= \frac{Weight\_transfer_{\_F}}{Weight\_transfer_{\_R}} \tag{4.14}$$

$$\propto \frac{Roll\_stiffness_{\_F}}{Roll\_stiffness_{\_R}} \quad or \quad \frac{Roll\_center\_height_{\_F}}{Roll\_center\_height_{\_R}} \tag{4.15}$$
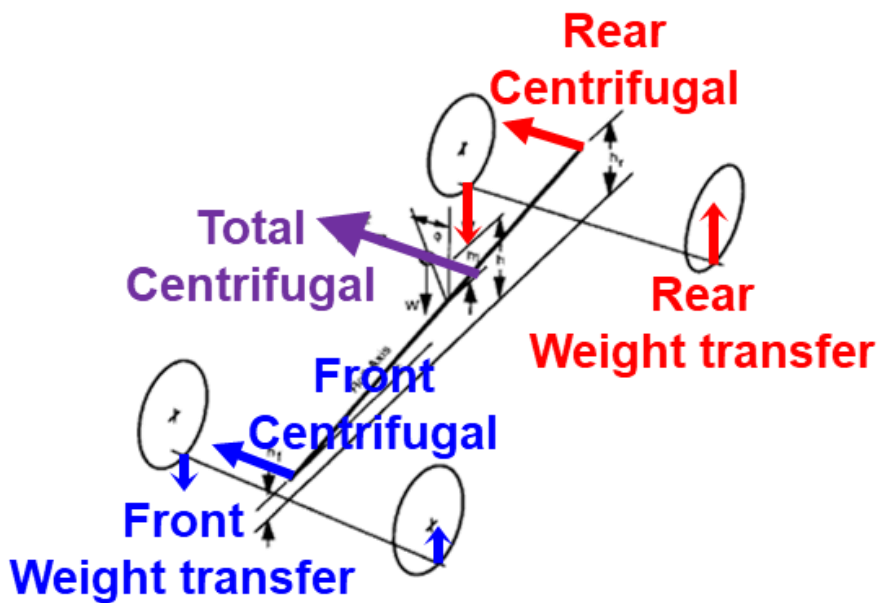
Figure 4.17. Weight transfer via Roll center height.

Chapter 5 . Control Logic for Oversteer Prevention

Oversteer prevention logic can reduce overshooting yaw motion during severe lane changes. The algorithm transmits driving torque from the outer wheel to the inner wheel in proportion to the level of excess yaw rate relative to the target yaw rate as shown in Figure 5.1.
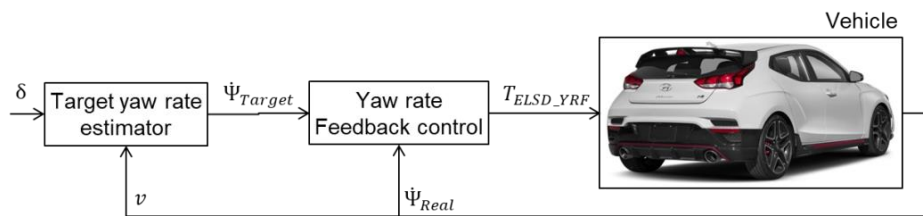
Figure 5.1. Diagram of control logic for oversteer prevention.

5.1. Yaw Rate Feedback Control

When the vehicle is in an oversteer state, the electronic limited slip differential (ELSD) is controlled as shown in Figure 5.2 to synchronize the front wheels' left-side and right-side speeds for creating a reverse moment to the vehicle yaw direction.
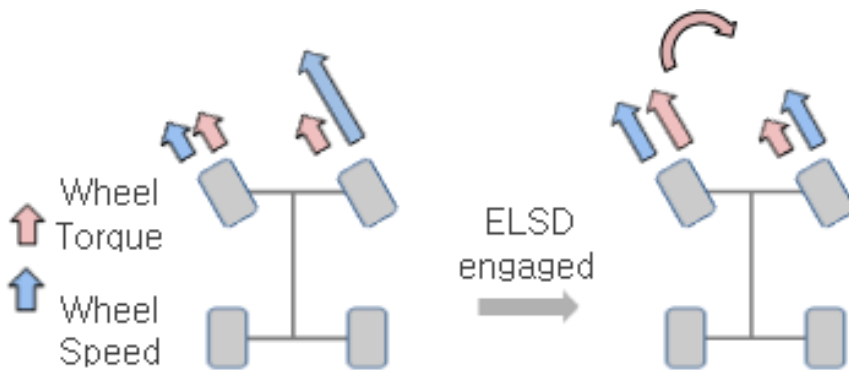
Figure 5.2. ELSD clutch operation during oversteer.

For the target yaw rate, the ideal steady state yaw rate gain by single track vehicle model is used to estimate the driver's intention. The ELSD clutch is engaged if the vehicle's yaw rate is greater than this estimated target yaw rate by driver's intention as shown in Figure 5.3 with the following equations.
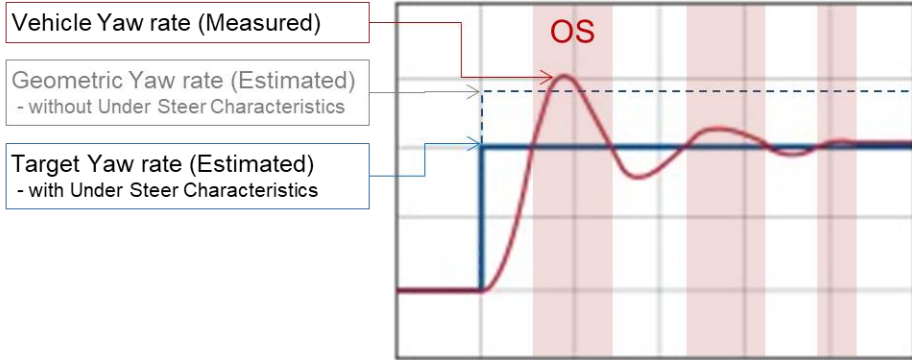
Figure 5.3. The concept of oversteer prevention control strategy.

Figure 5.3 represents yaw rate with respect to time. The geometric yaw rate is presented in a dotted black line. The target yaw rate is illustrated in a dark-blue line. A red line is the vehicle yaw rate.

$$\dot{\Psi}_{Target} = \frac{v}{L+K_{US}\cdot v^2} \cdot \delta = \frac{v}{L+(L/v_{ch})\cdot v^2} \cdot \delta \tag{5.1}$$

$$T_{ELSD\_YRF} = gain_{YRF} \cdot (\dot{\Psi}_{Real} - \dot{\Psi}_{Target}) \tag{5.2}$$

Where T_{ELSD_YRF} denotes the ELSD engaging torque by yaw rate feedback control, $\dot{\Psi}_{Target}$ denotes the target yaw rate from estimator, v denotes the vehicle speed, L denotes the wheel base, K_{US} denotes the understeer gradient, δ denotes steer angle of road wheel, v_{ch} denotes the characteristic speed, $\dot{\Psi}_{Real}$ denotes the real yaw rate from sensor.

Chapter 6 . Integrated Control of Electronic Stability Control (ESC), Electric Power-assist Steering (EPS), and Electronic Limited Slip Differential (ELSD)

6.1. Cooperative Control with ESC

In ESC side understeer control, rear-inner-wheel braking control is normally performed. In the case of excessive understeer, however, front-outer-wheel braking control is performed as shown in Figure 6.1.
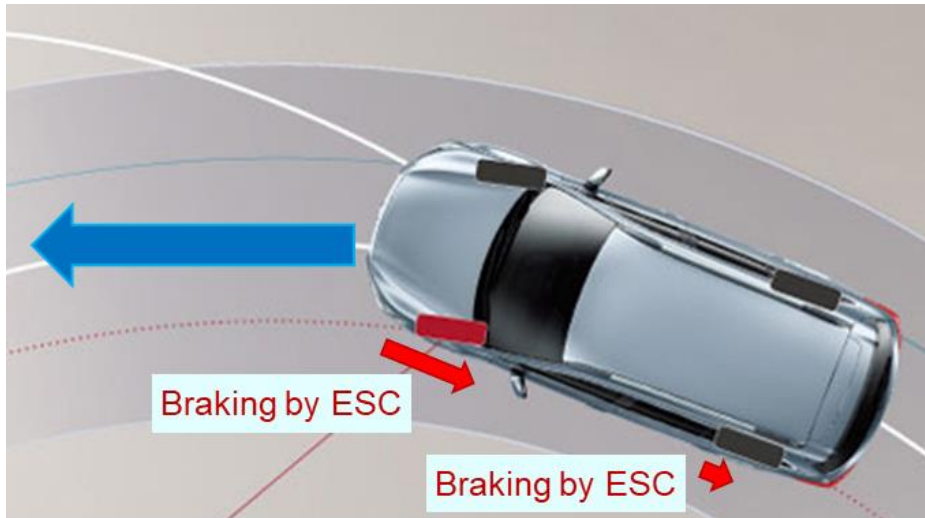
Figure 6.1. Front-outer-wheel braking control via ESC while excessive understeer.

However, with ELSD operation, the braking torque is applied on front-outer-wheel due to torque transfer by the engaged clutch of ELSD. This braking torque on front-outer-wheel may produce moment in direction of increasing understeer as shown in Figure 6.2
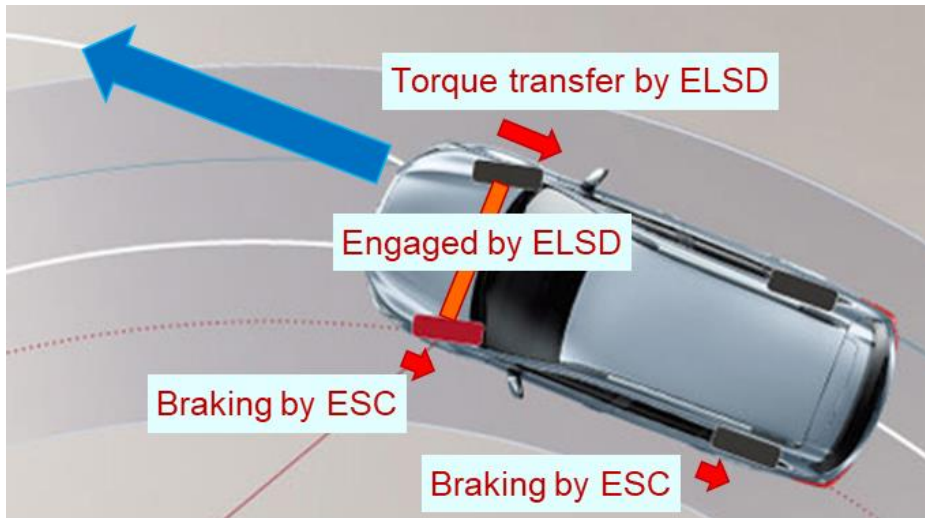
Figure 6.2. Braking torque is transferred to the opposite wheel by ELSD.

The reason is that engaging clutch of ELSD reduces the degree of freedom of front axle rotation from 2 to 1. That is, even if only the brake of one wheel is operated, braking torque is applied to the entire shaft that binds both wheels (Statically indeterminate). Therefore, the ratio of the right and the left distribution of the braking torque is proportional to their gripping level(≒ normal load distribution) as shown in Figure 6.3.

Without ELSD **2DOF**	- Each braking torque is apply to each wheel (Statically determinate)
With ELSD **1DOF**	- Each braking torque is apply to entire axle (Statically indeterminate) → Left/Right distribution is proportion to their grip ratio ($\fallingdotseq$ normal load distribution)
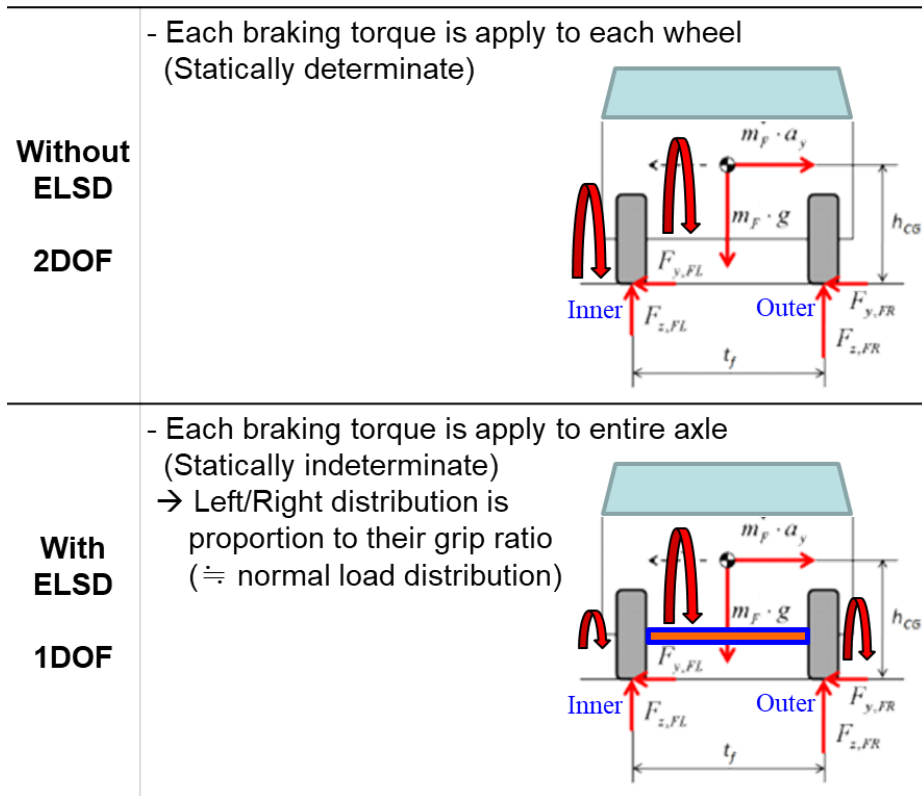
Figure 6.3. Inner wheel braking with engaging clutch of ELSD.

Likewise, when excessive oversteer occurred, ESC usually operates the front-outer-wheel brakes. But, with ELSD operation, the braking torque is applied on the front-inner-wheel due to the torque transfer by the engaged clutch of ELSD. This braking torque on front-inner-wheel may produce moment in direction of increasing oversteer,

Therefore, Cooperative control with ESC is configured so that the ESLD is activated during rear-wheel braking control, and ELSD is deactivated only

during front-wheel braking control as shown in Figure 6.4.
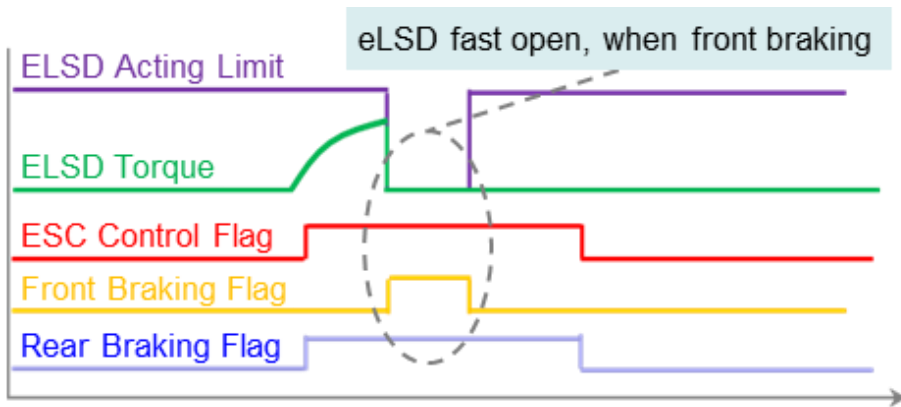
Figure 6.4. The concept of ELSD deactivated during front-wheel braking control.

Figure 6.4 represents ELSD torque and ESC control flag with respect time. The ELSD acting limit is presented in a violet line. The ELSD torque is illustrated in a green line. A red line is the ESC control flag. An orange line presents the front braking flag. The rear braking flag is presented in a blue line.

6.2. Cooperative Control with EPS

During acceleration in turn, the driving torque was increased in the outer wheel because the ELSD is activated. This torque difference generates torque steer problem in the current turning direction, because the equilibrium of forces acting on the steering rack is broken by the moment on the left and right kingpins. Originally, vehicle steering system is designed to apply proper return torque on steering wheel by aligning moment on tire. However the torque steer issue can change the return torque on steering wheel as shown in Figure 6.5.
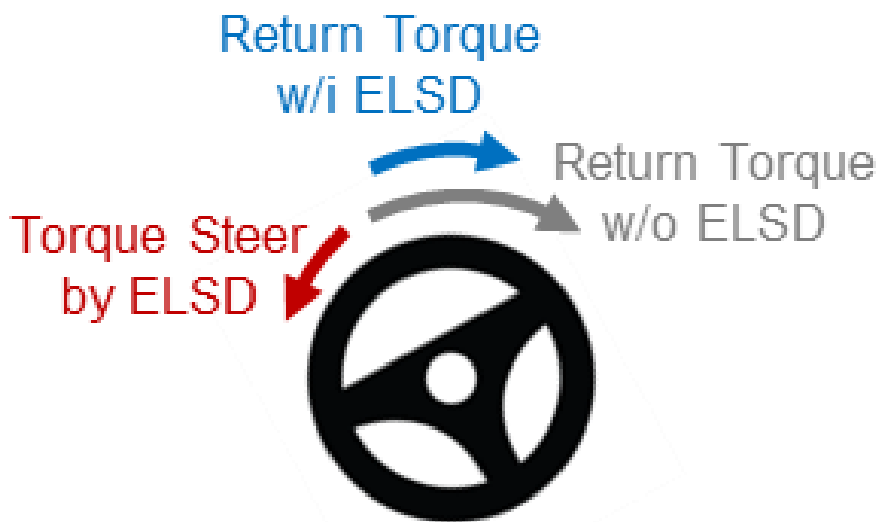
Figure 6.5. Reduction in return torque due to torque steer by ELSD.

The measurement results confirm that the driving torque of the outer

wheel is increased by ELSD operation upon the acceleration in turn, thereby reducing the outer tie-rod compressive force, thereby changing steering return torque as shown in Figure 6.6.
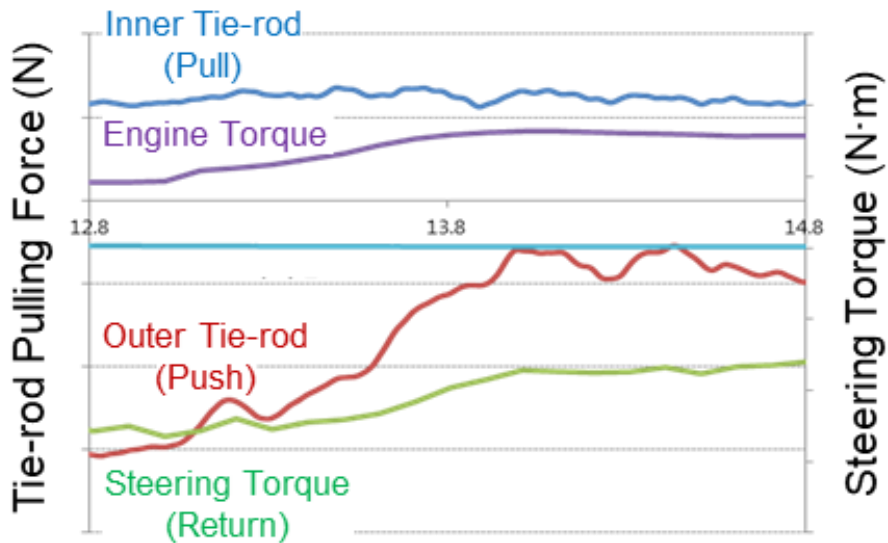
Figure 6.6. Measurement results related to reduced steering return.

Figure 6.6 represents steering angle, engine torque, tie-rod force, and steering torque with respect time. The engine torque is illustrated in a violet line. A blue line is the inner tie-rod force. A red line presents the outer tie-rod force. The steering torque is presented in a green line.

To resolve for this problem, the amount of ELSD torque-level is provide to EPS logic to calculate the additional motor torque for compensating the torque steer in control logic of EPS (Lee et al., 2019).

Chapter 7 .   Tire-road   Friction Estimation to Improve the Predictive Control

In order to reduce wheel speed feedback control intervention, the accuracy of the wheel spin predictive control can be improved with the prediction of the friction coefficient of the road surface. The prediction model for allowable driving force is based on the road friction coefficient, and for this, an accurate estimation of the tire-road friction is required. If a tire-road friction estimation error occurs, and the estimated tire-road friction value is smaller than the actual tire-road friction value as shown in Figure 7.1, the electronic limited slip differential (ELSD) control intervenes before the optimal time which means that the clutch is engaged even though the inner wheel spin is not occur. It can cause the opposite effect, which increases the understeer as like limited slip differential effect in no wheel spin condition. Conversely, if the tire-road friction is estimated to be larger than the actual tire-road friction, the amount of understeer control may be insufficient during inner wheel slip because of the delay in the ELSD operation.
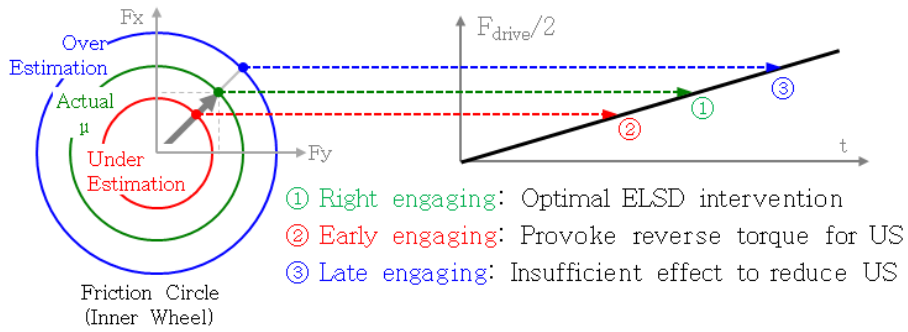
Figure 7.1. The concept of ELSD intervention time via friction estimation.

Figure 7.1 represents the driving force expected to be applied to each wheel with respect to time. The friction circles via friction estimation are represented using 3 lines. The exact estimation case is presented in a green line. The under estimation case is illustrated in a red line. A blue line is the over estimation case.

There are several methods for estimating tire-road friction. For the ELSD system to provide optimal control at the time of wheel slip, the friction value is estimated by real-time monitoring of the driving torque at the moment when wheel slip occurs as shown in in Figure 7.2 and the following equations.
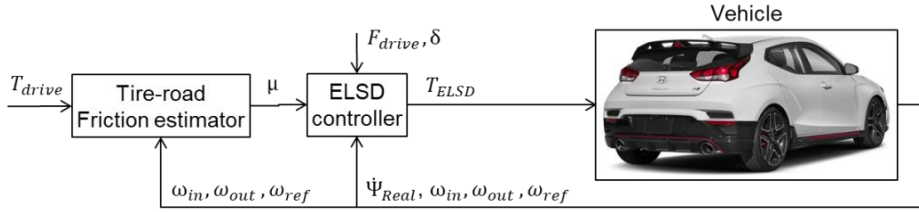
Figure 7.2. Control logic diagram for tire-road friction estimation.

$$\mu = \frac{\sqrt{F_x{}^2 + F_y{}^2}}{F_z} \qquad (7.1)$$

$$F_x = \frac{T_{drive} - I_{drive} \cdot \ddot{\theta}_{drive}}{R_{tire}} \qquad (7.2)$$

$$F_y = m \cdot a_y \qquad (7.3)$$

$$F_z = m \cdot g \qquad (7.4)$$

Where I_{drive} denotes the rotational inertia of driveline, $\ddot{\theta}_{drive}$ denotes the rotational acceleration of driveline.

Because the electronic stability control (ESC) system operates on the region of the grip limit, the friction coefficient calculated at this time is close to the actual friction value. However, It is necessary to estimate the friction coefficient from ELSD at all times while in operation.

Therefore, on the region of the grip limit (unstable wheel slip region that is above the wheel slip criterion value), the instantaneous calculated value is

estimated to be the real-time friction coefficient, as in ESC as shown in Table 7.1.

Table 7.1. Tire-road friction values according to the wheel slip rate category.

Situation	Mu Estimation	Low-Pass Filter
Stable (Big Slip Ratio)	$\max[\mu(n-1), \mu(n)]$	Cutoff Frequency High
Unstable (Small Slip Ratio)	$\mu(n)$	Cutoff Frequency Low

μ(n): Friction coefficient calculated in real time

μ(n-1): Friction coefficient calculated just before

In other regions, minor speed differences occur between the driving wheels and the non-driving wheels during not much acceleration. At these times, the engine torque is low, which corresponds to small acceleration situations. Therefore, the calculated friction value is continuously at a low level. Hence, the stable region (stable wheel slip region, below the wheel slip criterion value) was defined. In this region, the friction coefficient is estimated as the larger of the current friction coefficient and the previous friction coefficient.

The above method was used to increase the tire-road friction estimation accuracy, while also resolving the problem of underestimating the tire-road friction value during normal grip driving conditions as shown in Figure 7.3 and Table 7.2.
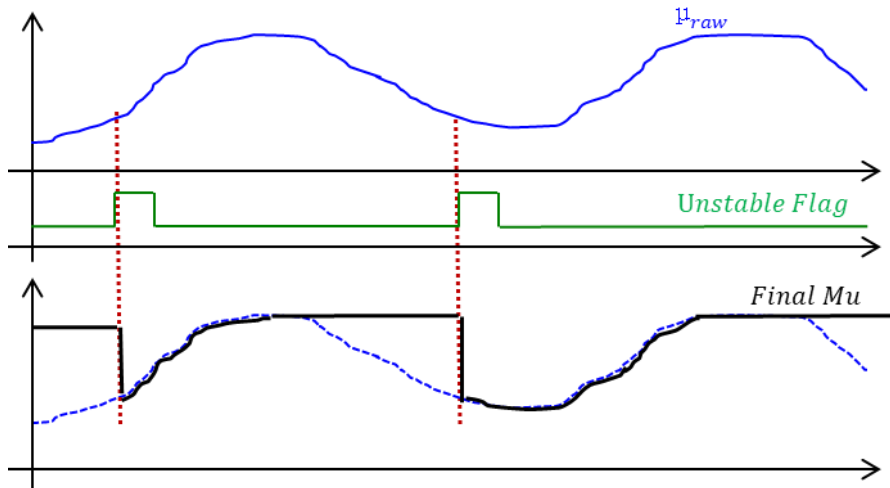
63

Figure 7.3. Tire-road friction estimation results.

Figure 7.3 represents unstable status flag and friction value with respect time. The unstable status flag is presented in a green line. The friction coefficient calculated in real time is illustrated in a blue line. A black line is the friction coefficient estimated at the end

.

Table 7.2. Tire-road friction estimation results compared to actual tire-road friction.

PG	Boxberg PG				Nürburgring
Road Surface	Wet Asphalt	Wet Concrete	Wet Basalt	Wet Urethane	Dry Asphalt
Measuring	0.6	0.4	0.2	0.2	0.9
Simulation	0.6	0.4	0.3	0.2	0.9

Friction estimates by this method are suitable for ELSD due mainly to the racing track driving characteristic in which ELSD is effective.

- Use longitudinal or lateral acceleration largely.

- Repeat the designated course.

Chapter 8 . Validation: Vehicle Tests

The proposed algorithm has been validated through vehicle tests. A C-segment high-performance vehicle model (Veloster N) was utilized as the test vehicle. The vehicle is one of the mass-produced vehicles with the proposed algorithm using electronic limited slip differential (ELSD). As a main computing controller, XC2060N which is manufactured by Infineon Technologies AG, is utilized. The specifications of the vehicle are as shown in Table 8.1.

The scenario is set to closed-loop acceleration in a turn and closed-loop double lane change. For comparison, two different conditions were investigated: (1) 'ELSD on' by proposed algorithm; and (2) 'ELSD off'.

Table 8.1. The specifications of the test vehicle.

Category	Unit	Content
Overall length	mm	4,265
Overall width	mm	1,810
Overall height	mm	1,395
Wheelbase	mm	2,650
Wheel tread front	mm	1,555
Wheel tread rear	mm	1,564
Curb weight	kg	1,415
Engine type	-	Turbo Gasoline Direct Injection
Engine valve train	-	DOHC 16-valve with E-CVVT[1]
Engine displacement	ml	1,998
Engine power	PS / rpm	275 / 6,000
Engine torque	kg·m / rpm	36 / 1,450~4,700
Transmission type	-	6-speed manual
Driving Type	-	Front Wheel Drive
Suspension front	-	MacPherson Strut with ECS[2]
Suspension rear	-	Multi-link with ECS
Tire	-	235/35 R19, Summer Performance tires

(1) Continuous Variable Valve Timing

(2) Electronic Controlled Suspension

8.1. Configuration of Vehicle Tests

In order to conduct the vehicle test, the test vehicle has been built with some equipment. The test vehicle model is A C-segment high-performance vehicle model (Veloster N) of Hyundai Motor Company.

A steering robot, SR35 which is manufactured by AB Dynamics, is installed in the test vehicle. The steering input is manipulated by transmitting the control command values to SR35. The configuration of the test vehicle with steering robot is presented in Figure 8.1

Figure 8.1. The configuration of the test vehicle with steering robot.

A GPS-aided inertial measurement system device, RT3000 which is manufactured by Oxford Tech., is employed to measure vehicle motion such as vehicle displacement of each direction, vehicle velocity of each direction,

vehicle acceleration of each direction, and body side slip angle. The configuration of the inertial measurement system in test vehicle is presented in Figure 8.2

Figure 8.2. The configuration of the inertial measurement system.

Spinning Wheel Integrated Force Transducer, SWIFT Evo   which   is manufactured by MTS, is installed to measure not only driving torque but also braking torque. The configuration of wheel force transducer system in test vehicle is presented in Figure 8.3

Figure 8.3. The configuration of wheel force transducer system in test vehicle.

A data acquisition system, DEWE-211 which is manufactured by DEWETRON GmbH, is employed to record the signal from inertial measurement system and wheel force transducer system conditions as shown in Figure 8.4.

Figure 8.4. Data acquisition system, DEWE-211
(courtesy of DEWETRON GmbH).

The data acquisition software, DEWESoft which is manufactured by DEWESoft, is used to acquire data with DEWE-211. The configuration of measurement data acquisition system in test vehicle is presented in Figure 8.5

Figure 8.5. The configuration of measurement data acquisition system.

8.2. Closed-loop Acceleration in A Turn

Closed-loop acceleration in a turn was conducted to investigate the understeer prevention algorithm. The turning radius was 100 m, and the initial speed was 50 km/h.

Test results are presented in Figure 8.6, 8.7, 8.8, 8.9, 8.10, 8.11, 8.12, 8.13, 8.14, and 8.15. Overall vehicle states are illustrated in Figure 8.6, 8.7, 8.8, and 8.9. The cross plot of lateral acceleration/steering wheel angle and steering wheel angle/yaw rate are presented in Figure 8.10 and 8.11. The ELSD torque input and wheel speed difference are illustrated in Figure 8.12, 8.13, 8.14, and 8.15. A positive yaw moment means that the vehicle rotating moment leads to a left turn.

Compared to the 'ELSD off' condition, the vehicle speed increment of the 'ELSD on' condition was larger as shown in Figure 8.7. This is due to no spin of the left wheel by engaging the ELSD clutch as depicted in Figure 8.12 and 8.13. Therefore, the torque on the left that is lost was transferred to the right as illustrated in Figure 8.14. In addition, 'ELSD on' condition generated a bigger yaw rate and lateral acceleration than 'ELSD off' condition while steering wheel angle was similar level as shown in Figure 8.6, 8.8, and 8.9. This performance is more clearly expressed in the cross plot as depicted in Figure 8.10 and 8.11. This is due to larger yaw moment by the front wheel torque difference as illustrated in Figure 8.15.

In summary, the proposed algorithm could prevent excessive understeer of the vehicle during acceleration in turn. The lateral acceleration via same steering wheel angle after acceleration in turn was increased by 10%. Moreover, the proposed algorithm showed improved acceleration performance during acceleration in turn. The vehicle speed after acceleration in turn was increased by 7%.
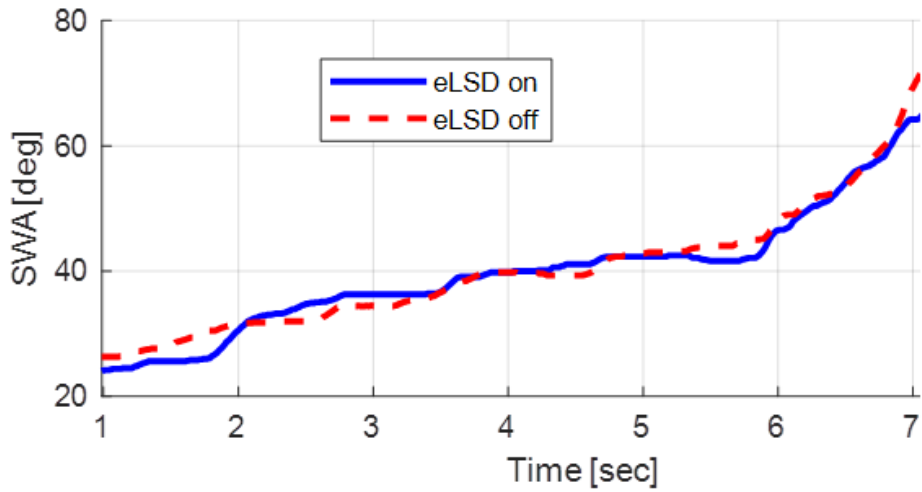
Figure 8.6. R-100m acceleration in a turn (closed-loop) test on dry asphalt
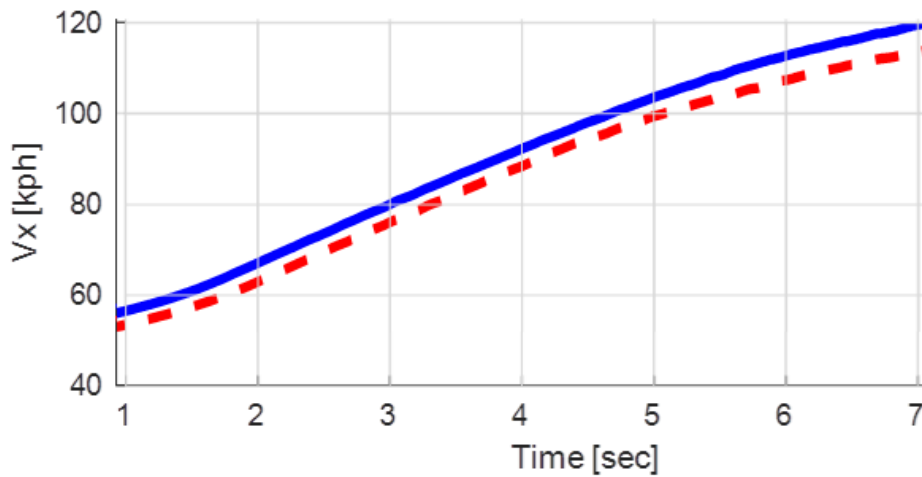: Steering wheel angle

Figure 8.7. R-100m acceleration in a turn (closed-loop) test on dry asphalt
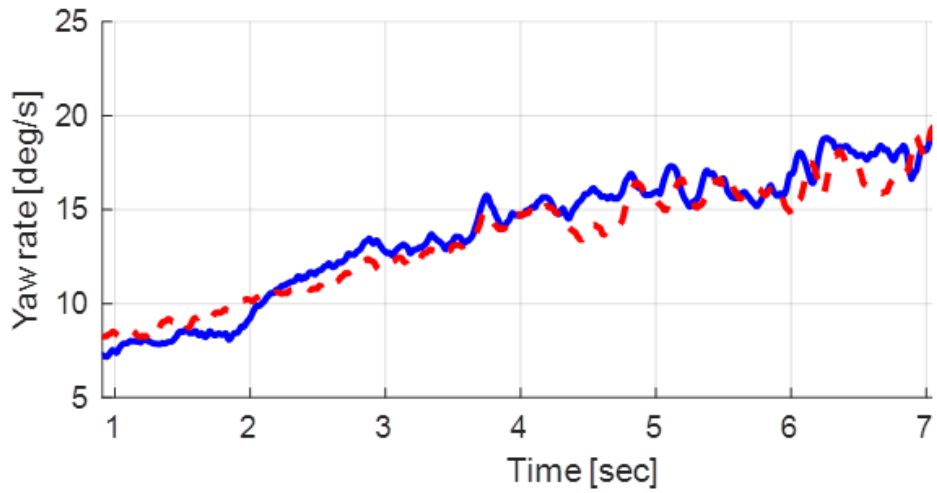: Longitudinal velocity.

Figure 8.8. R-100m acceleration in a turn (closed-loop) test on dry asphalt
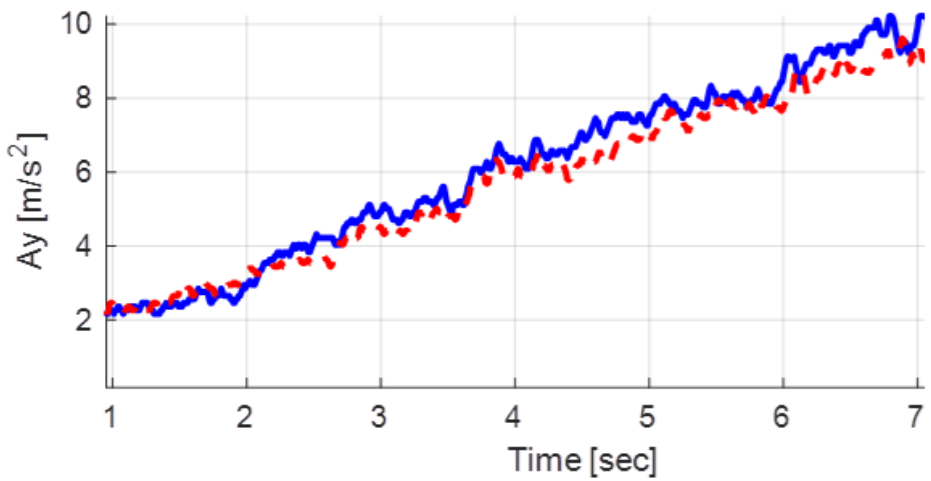: Yaw rate.

Figure 8.9. R-100m acceleration in a turn (closed-loop) test on dry asphalt
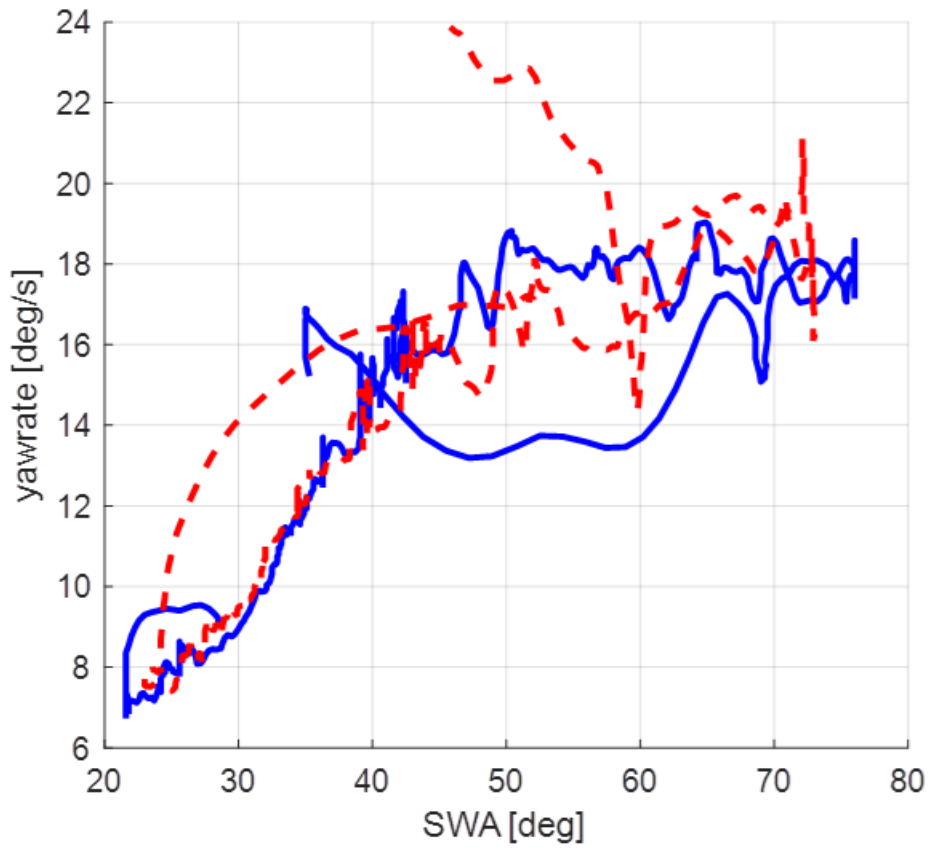: Lateral acceleration.

Figure 8.10. R-100m acceleration in a turn (closed-loop) test on dry asphalt
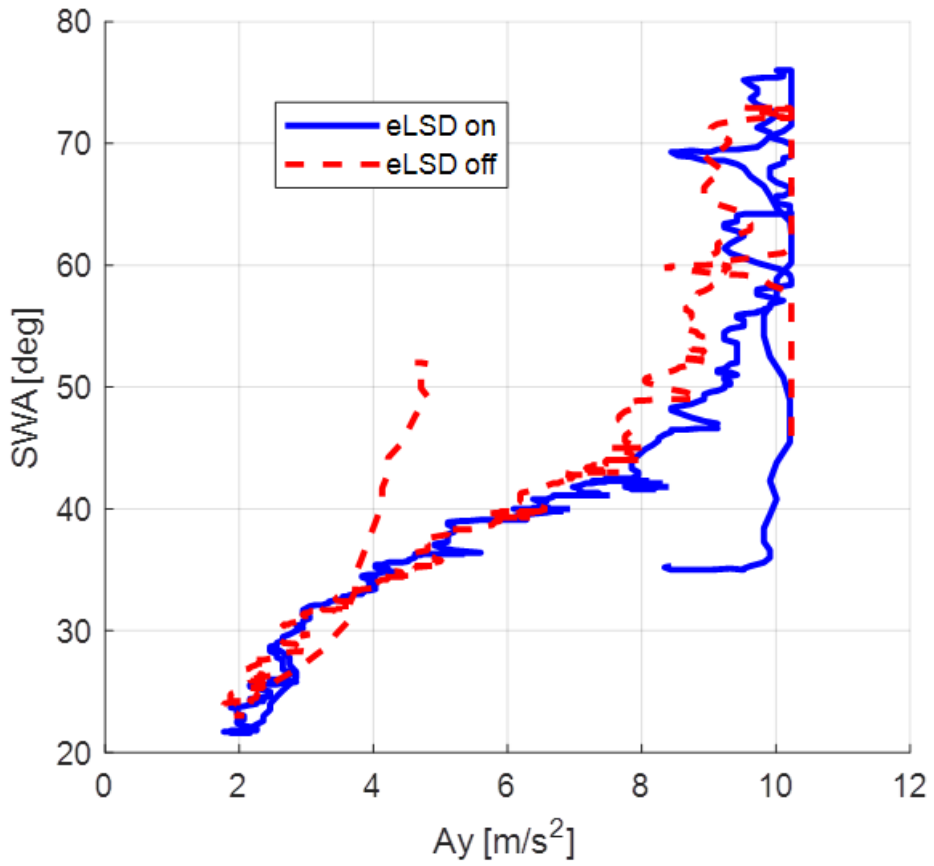: Steering wheel angle vs Yaw rate.

Figure 8.11. R-100m acceleration in a turn (closed-loop) test on dry asphalt
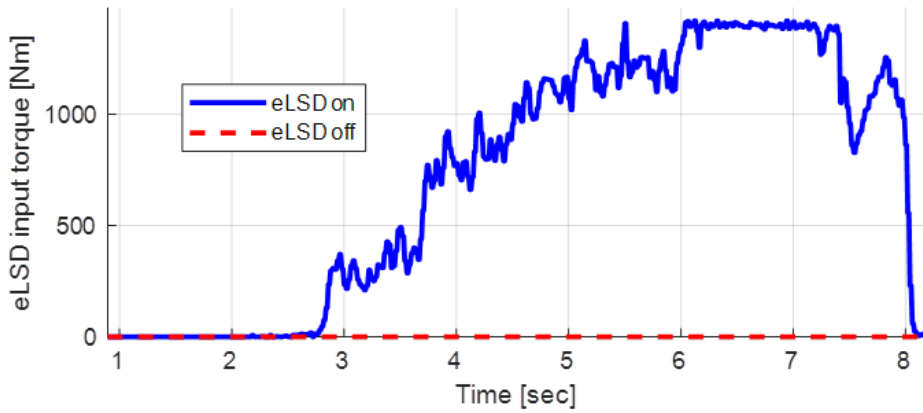: Lateral acceleration vs Steering wheel angle.

Figure 8.12. R-100m acceleration in a turn (closed-loop) test on dry asphalt
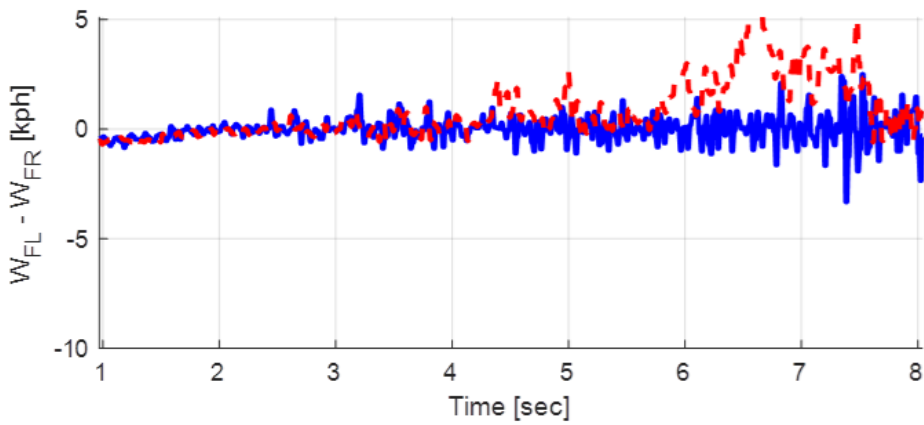: ELSD torque input.

Figure 8.13. R-100m acceleration in a turn (closed-loop) test on dry asphalt
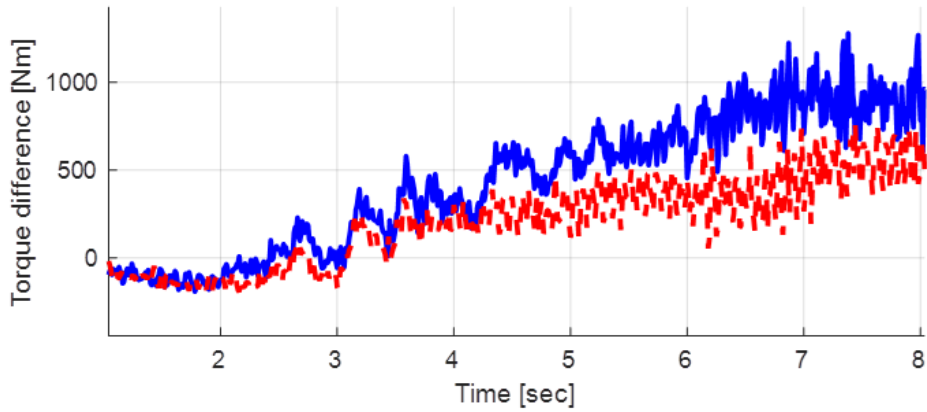: Wheel speed difference.

78

Figure 8.14. R-100m acceleration in a turn (closed-loop) test on dry asphalt
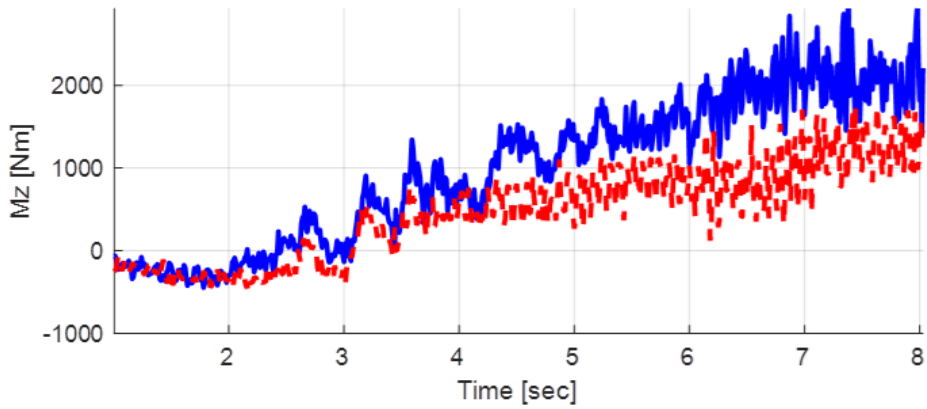: Wheel torque difference.

Figure 8.15. R-100m acceleration in a turn (closed-loop) test on dry asphalt
: Yaw moment by driving wheel.

8.3. Closed-loop Double Lane Change

Closed-loop double lane change was conducted to investigate the oversteer prevention algorithm. The initial speed was 120 km/h.

Test results are presented in Figure 8.16, 8.17, 8.18, 8.19, 8.20, 8.21, 8.22, 8.23, 8.24, 8.25, 8.26, and 8.27. Overall vehicle states are illustrated in Figure 8.16, 8.17, 8.18, and 8.19. The torque and speed of each wheel is presented in Figure 8.20, 8.21, 8.22, and 8.23. The ELSD torque input and wheel speed difference are illustrated in Figure 8.24, 8.25, 8.26, and 8.27. Positive yaw moment means that vehicle rotating moment leads to a left turn.

The vehicle speed of the 'ELSD off' condition at the second left turn was reduced compared to the 'ELSD on' condition as shown in Figure 8.17. This is due to the need for deceleration to follow the course as depicted in Figure 8.20, 8.21, 8.22, and 8.23. Nevertheless, the yaw rate of the 'ELSD on' condition at the second left turn was smaller versus 'ELSD off' condition while lateral acceleration at that time was similar level as illustrated in Figure 8.18 and 8.19. This is due to a larger yaw damping moment by the front wheel torque difference as shown in Figure 8.27.

In summary, the proposed algorithm could prevent excessive oversteer of the vehicle during double lane change. The yaw rate over-shoot at the same lane change was reduced by 25%. Moreover, the proposed algorithm also showed improved speed through the double lane change course. The exit speed after double lane change was increased by 10%.
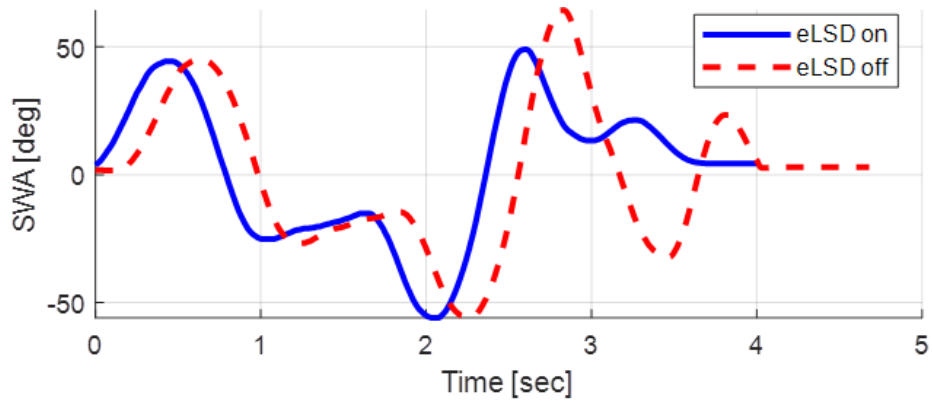
Figure 8.16. Double lane change (closed-loop) test on dry asphalt
: Steering wheel angle.

Figure 8.17. Double lane change (closed-loop) test on dry asphalt
: Longitudinal velocity.

Figure 8.18. Double lane change (closed-loop) test on dry asphalt
: Yaw rate.

Figure 8.19. Double lane change (closed-loop) test on dry asphalt
: Lateral acceleration.

Figure 8.20. Double lane change (closed-loop) test on dry asphalt
: Front left wheel torque.

Figure 8.21. Double lane change (closed-loop) test on dry asphalt
: Front right wheel torque.

Figure 8.22. Double lane change (closed-loop) test on dry asphalt
: Front left wheel speed.

Figure 8.23. Double lane change (closed-loop) test on dry asphalt
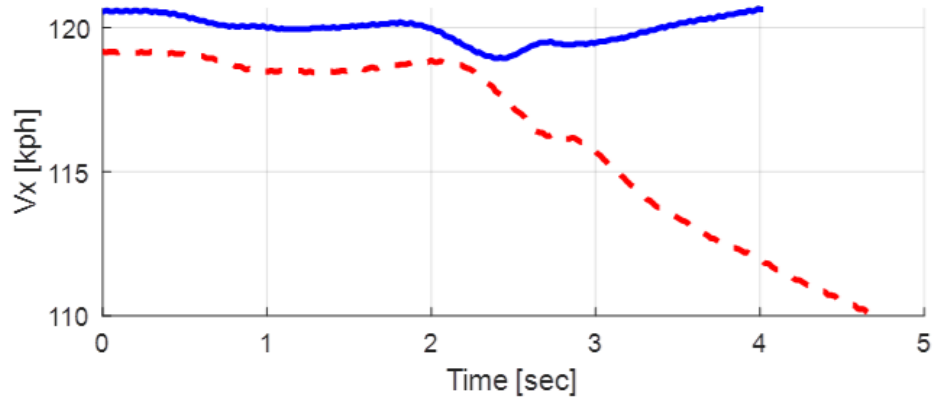: Front right wheel speed.

Figure 8.24. Double lane change (closed-loop) test on dry asphalt
: ELSD torque input.
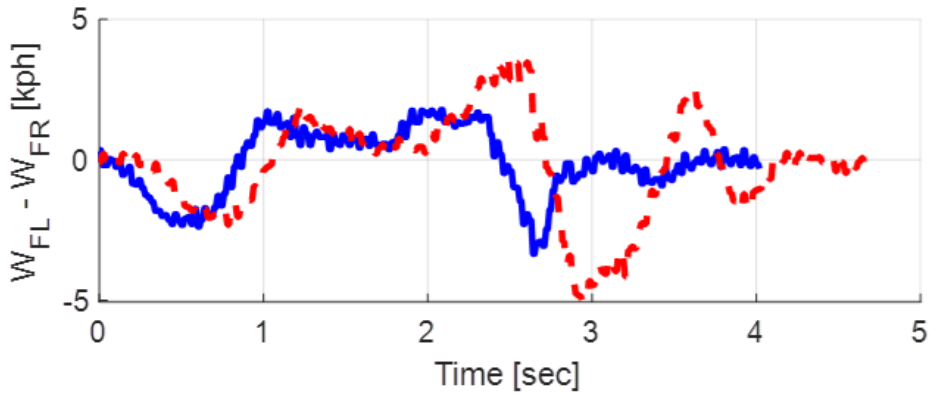
Figure 8.25. Double lane change (closed-loop) test on dry asphalt
: Wheel speed difference.
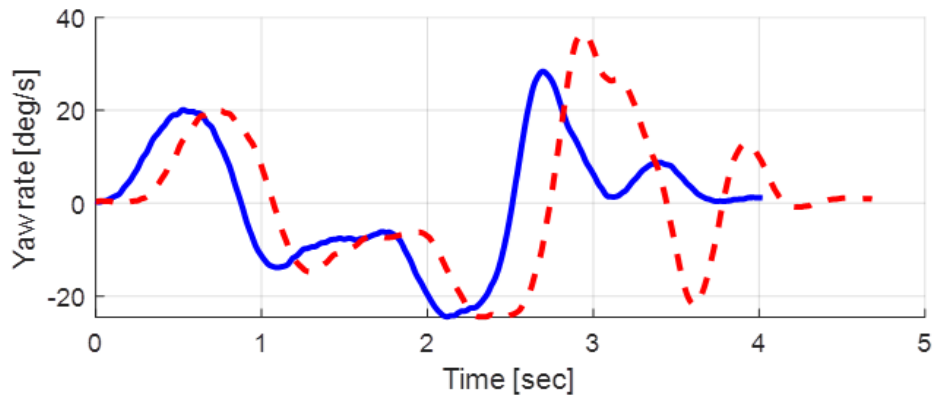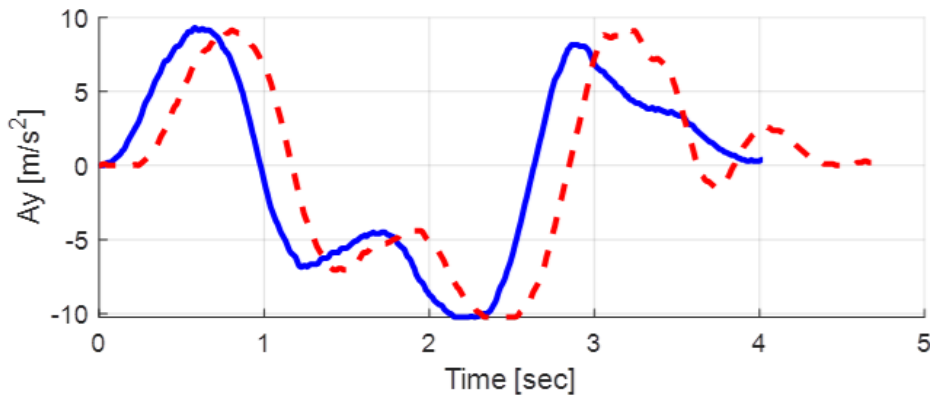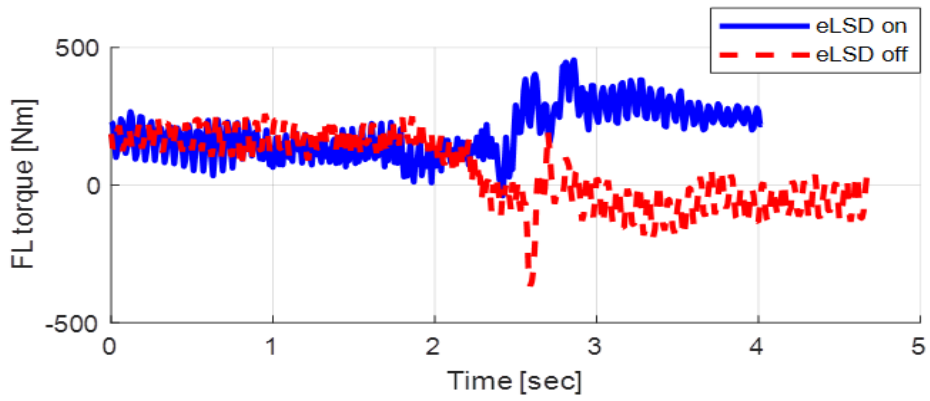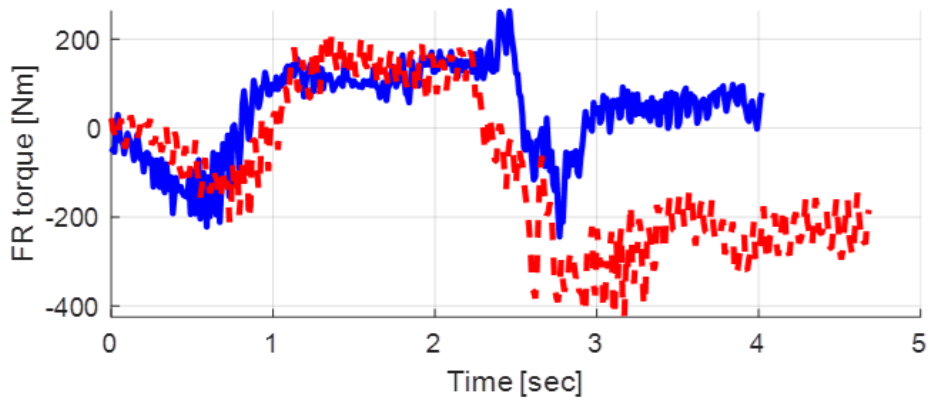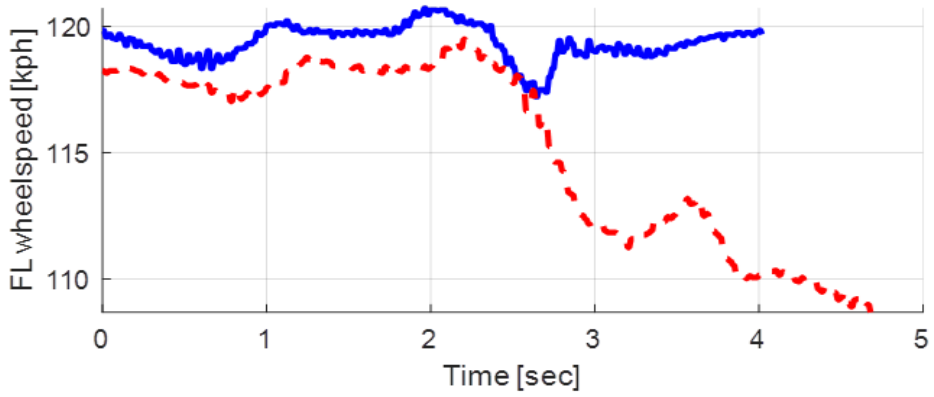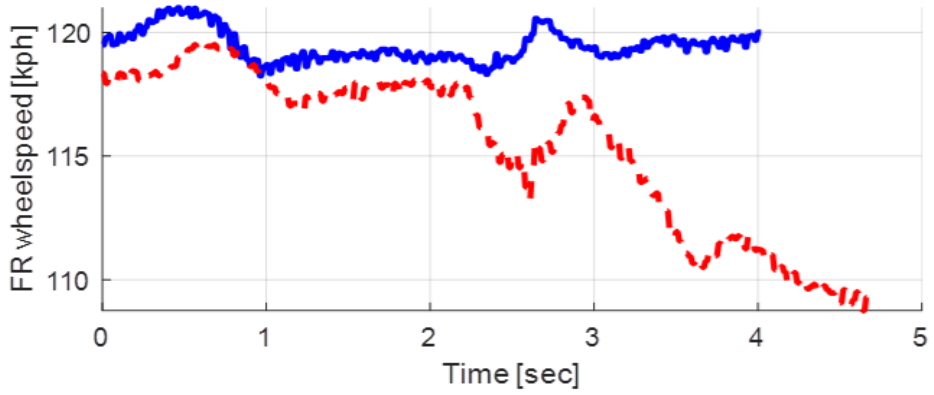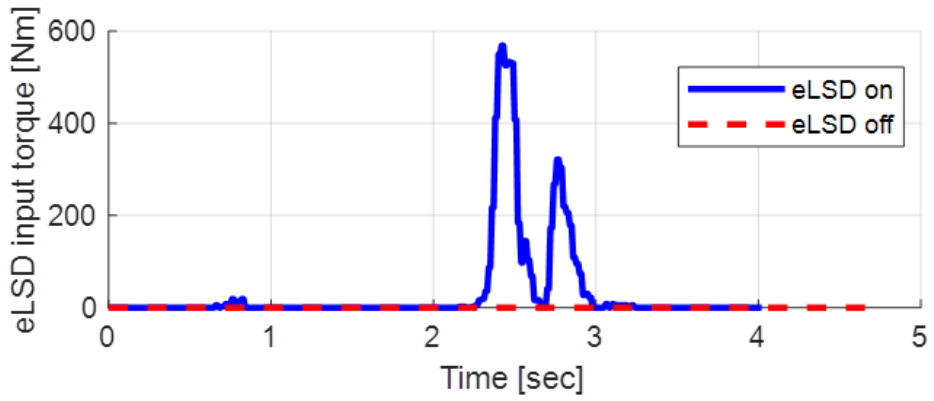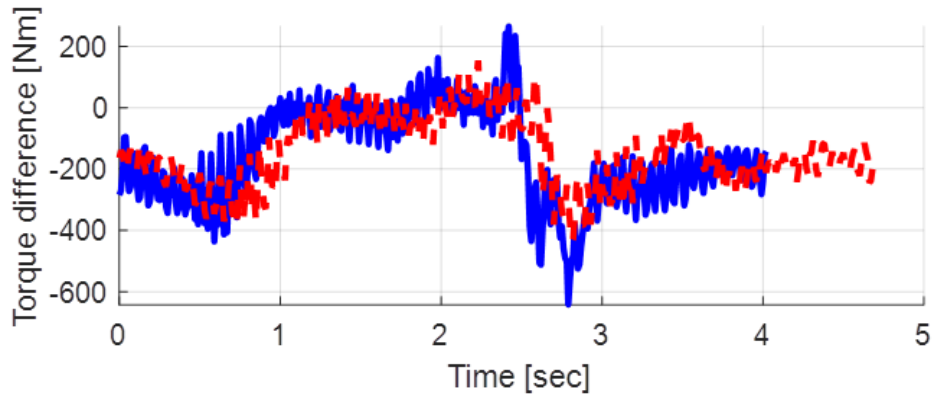
Figure 8.26. Double lane change (closed-loop) test on dry asphalt
: Wheel torque difference.
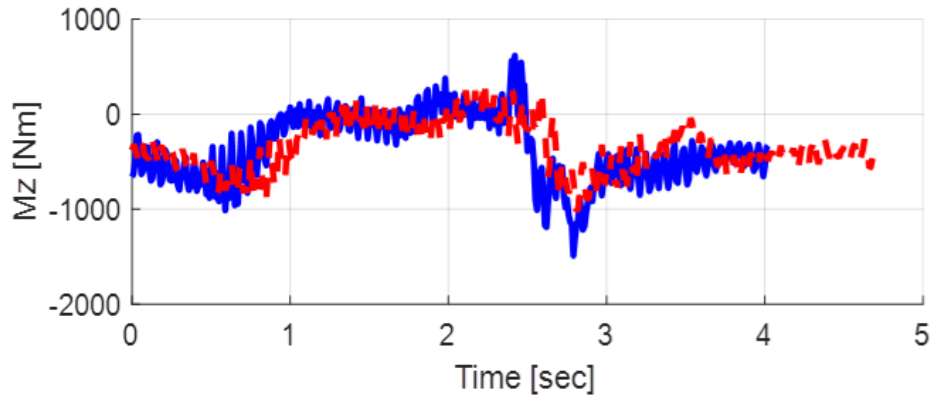
Figure 8.27. Double lane change (closed-loop) test on dry asphalt
: Yaw moment by driving wheel.

8.4. Performance Comparison with Competitor

Closed-loop acceleration in a turn was conducted for comparison with competitor, Volkswagen Golf (Mk7) GTI with ELSD. The turning radius was 100 m, and the initial speed was 50 km/h.

Test results are presented in Figure 8.28 and 8.29. Steering wheel angle, ELSD operation torque, yaw rate is illustrated in Figure 8.28. The cross plot of y displacement and x displacement is presented in Figure 8.29.

Compared to the 'Volkswagen', the yaw rate of the 'Hyundai' was larger via a smaller steering wheel angle as depicted in Figure 8.28(c), 8.28(a). This is due to a larger engaging torque via their ELSD clutch as shown in Figure 8.28(b). In addition, it can be seen that Hyundai follows the turning trajectory better than Volkswagen as illustrated in Figure 8.29.

In summary, the proposed algorithm could prevent excessive understeer of the vehicle during acceleration in turn than competitor. Therefore, when the proposed algorithm is applied with the ELSD, the same corner can be delivered faster than the vehicle equipped with the competitor's ELSD.
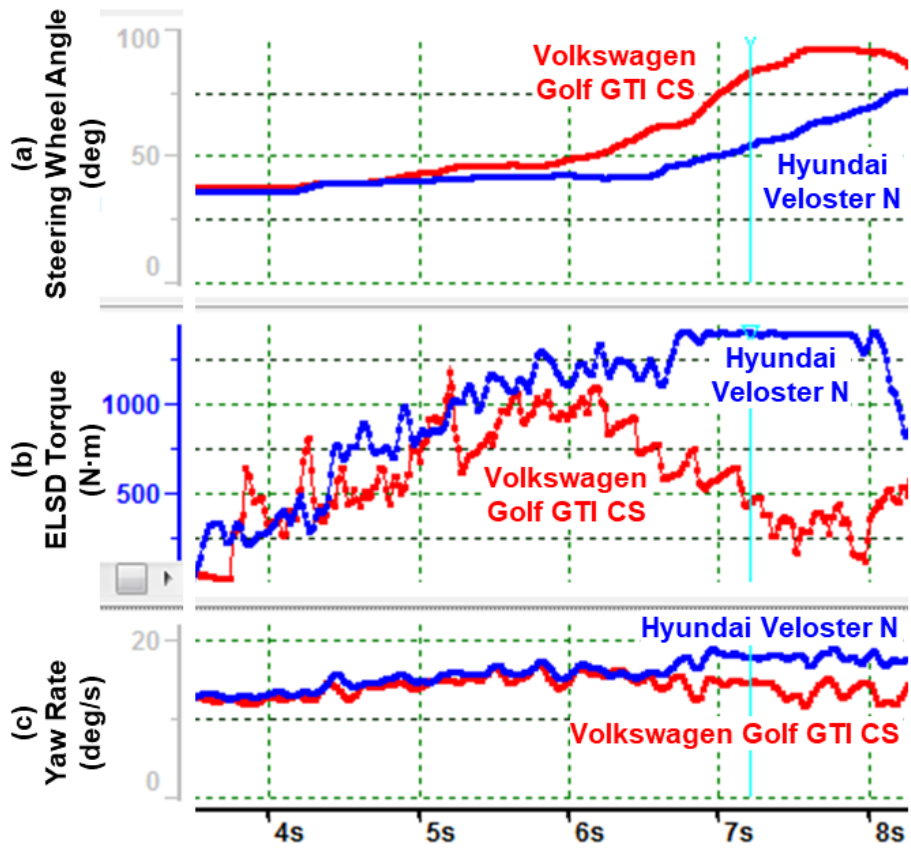
Figure 8.28. R-100m acceleration in a turn (closed-loop) test with competitor : (a) Steering wheel angle, (b) ELSD torque, (c) Yaw rate.
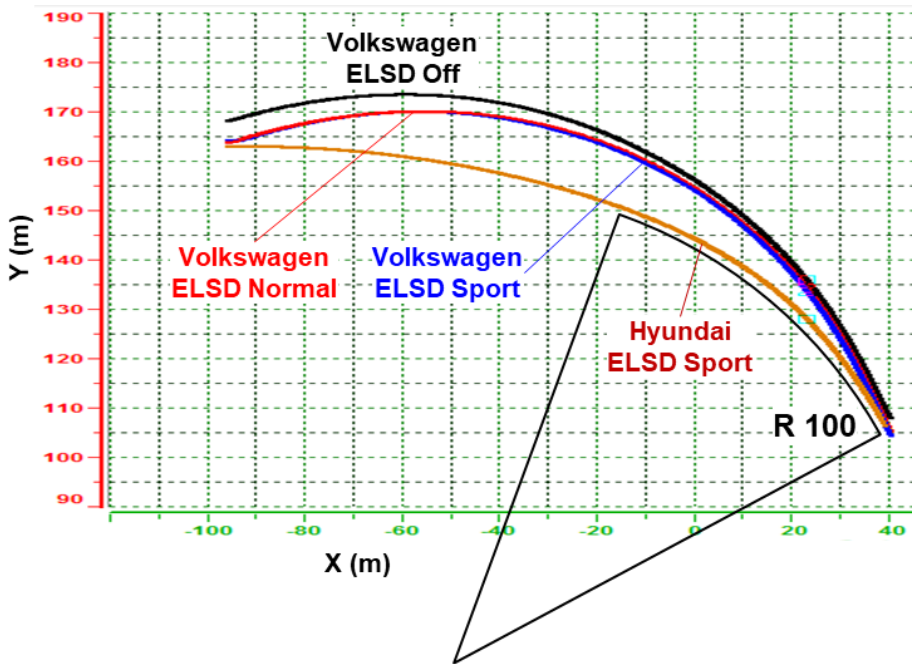
Figure 8.29. R-100m acceleration in a turn (closed-loop) test with competitor
: The cross plot of y and x displacement.

Chapter 9 . Conclusions and Future Works

A predictive control strategy for improved handling and acceleration performance of front-wheel-drive high performance vehicles with electronic limited slip differential has been described. the disadvantages of front-wheel-drive high-performance vehicles can be overcome through the proposed control strategies. The proposed algorithm is capable of implementing a higher level of torque bias ratio than mechanical helical-gear-type mechanical limited slip differential (MLSD) could be implemented. And the side effect of MLSD was fundamentally resolved using the function that can control this differential limiting function (so that it is only applied when needed). In summary, the proposed algorithm could prevent excessive understeer of the vehicle during acceleration in turn. The lateral acceleration via identical steering wheel angle after acceleration in turn was increased by 10%. Moreover, the proposed algorithm shows improvement in terms of accelerating performance while acceleration in turn. The vehicle speed after acceleration in turn was increased by 7%.

Oversteer can be overcome through engaging the front-wheel drive shaft upon detecting oversteer, which enables the vehicle to follow a faster and more stable course. In summary, the proposed algorithm can prevent excessive oversteer of the vehicle during double lane change. The yaw rate

over-shoot at the same lane change was reduced by 25%. Moreover, the proposed algorithm also showed improved speed through the double lane change course. The exit speed after double lane change was increased by 10%.

The adverse effects of simultaneously engaging the electronic stability control (ESC) and electronic limited slip differential (ELSD) were overcome through cooperative control with the electronic stability control system.

The sensation of difference in steering caused by a change in proper return torque of steering during ELSD operation was improved by providing the amount of ELSD torque-level to the Electric Power-Assist Steering logic. The system could then calculate the additional motor torque for compensating the torque steer in the control logic of the Electric Power-Assist Steering.

Ultimately, ELSD control reduced the lap time on the Nürburgring Nordschleife track by 7 sec versus no ELSD control.

The proposed algorithm was verified through patents on the control method and friction estimation method for the research novelty (Woo et al., 2019; Woo et al., 2019). The ELSD with the proposed algorithm was then applied to mass production. This approach received positive feedback from international media due to the significant improvements in vehicle performance via ELSD. The system with the proposed algorithm also was won the IR52 Jang Young-shil Award for its technological importance, originality, economic value and technical spill-over effect (Hyundai Motors Company 2020).

Although the approach presented in this study has significantly improved the performance of agility during acceleration in turn for front-wheel-drive high performance vehicles as well as the performance of vehicle stability,

91

there are still elements to improve. The handling performance is influenced not only by a torque distribution characteristic but also a suspension characteristic such as toe and camber of wheel. Therefore, it is expected that the vehicle handling performance can be improved through an optimization of suspension characteristic with ELSD. Tire characteristic will be also analyzed to enhance ELSD operation.

Since electric vehicles begin to need of high-performance characteristic, the proposed algorithm can be utilized as a foundation for the ELSD of electric vehicles. As the electric motor has rapid torque increase, the control systems should cope with the wheel spin prevention via model-based predictive control. The electric vehicle ELSD algorithm that employs the proposed algorithm as a basis is the topic of our future researches.

Bibliography

Uematsu, K. and Gerdes, J. C. (2002). A comparison of several sliding surfaces for stability control. In Proc. AVEC.

Heißing, B. and Metin, E. (Eds.). (2010). Chassis Handbook: Fundamentals, Driving Dynamics, Components, Mechatronics, Perspectives. Springer Science & Business Media.

Chen, Y., Hedrick, J. K., and Guo, K. (2013). A novel direct yaw moment controller for in-wheel motor electric vehicles. Vehicle System Dynamics, 51(6), 925–942.

Song, P., Tomizuka, M., and Zong, C. (2015). A novel integrated chassis controller for full drive-by-wire vehicles. Vehicle System Dynamics, 53(2), 215–236.

Joa, E. et al. (2017). A tyre slip-based integrated chassis control of front/rear traction distribution and four-wheel independent brake from moderate driving to limit handling. Vehicle System Dynamics, 1–25.

Lutz, A. et al. (2017). Simulation methods supporting homologation of electronic stability control in vehicle variants. Vehicle System Dynamics, 1–66.

Platteau, R. et al. (1995). Traction and handling safety synergy of combined torsen differential and electronic traction control. ImechE , 1995, CA98/30/144.

Velenis, E. et al. (2011). Steady-state drifting stabilization of RWD vehicles. Control Engineering Practice, 19, 11, 1363-1376.

Goh, Jonathan Y. and Gerdes, J. Christian (2016). Simultaneous Stabilization and Tracking of Basic Automobile Drifting Trajectories. 2016 IEEE Intelligent Vehicles Symposium, (IV).

Joa, E. et al. (2020). A new control approach for automated drifting in consideration of the driving characteristics of an expert human driver. Control Engineering Practice, 96, March 2020, 104293.

Shin, S. and Bowerman, W. (2002). An evaluation of torque bias and efficiency of Torsen differential. SAE Transactions, 2002, 2002-01-1046.

Woo, S. et al. (2007). Solution for the torque steer problem of a front-wheel drive car with a high-torque engine in vehicle development stages. SAE Technical Paper, 2007, 2007-01-3656.

Sasaki, H. et al. (1994). Development of an electronically controlled limited slip differential system. JSAE Review, 15 (1994), 341-365.

Piyabongkarn, D. et al. (2006). Dynamic modeling of torque-biasing devices for vehicle yaw control. SAE Technical Paper, 2006, 2006-01-1963.

Hancock, M. J. et al. (2007). Yaw motion control via active differentials. Transactions of the Institute of Measurement and Control, 29, 2 (2007) 137–157.

Piyabongkarn, D. et al. (2007). On the use of torque-biasing systems for electronic stability control: Limitations and possibilities. IEEE Transactions on Control Systems Technology, Vol. 15, No. 3, May 2007.

Damrongrit et al. (2010). Active Driveline Torque-Management Systems. IEEE Control Systems Magazine, August 2010, 86–102.

Assadian, F. et al. (2010). Development of a control algorithm for an active limited slip differential. Pro-ceedings of the 10th International Symposium on Advanced Vehicle Control (AVEC), Loughborough, UK, 22nd-26th August, 55-60.

Mashadi, B. et al. (2011). Vehicle stability enhancement by using an active differential. Proc. IMechE, Vol. 225 Part I: J. Systems and Control Engineering.

Rubin, D. and Arogeti, S. A. (2015). Vehicle yaw stability control using active limited slip differential via model predictive control methods. Vehicle System Dynamics, 53:9, 1315–1330.

Kinsey, J. (2004). The advantages of an electronically controlled limited slip differential. SAE Technical Paper, 2004, 2004-01-0861 .

Piyabongkarn, D., Lew, J., Grogg, J., and Kyle, R. (2006). Stability-enhanced traction and yaw control using electronic limited slip differential. SAE Technical Paper, 2006, 2006-01-1016.

Fox, M. and Grogg, J. (2012). Development of front-wheel-drive ELSD for Efficient Performance and Safety. SAE Technical Paper, 2012, 2012-01-0305.

Morselli, R. et al. (2006). Detailed and reduced dynamic models of passive and active limited-slip car differentials. Mathematical and Computer Modelling of Dynamical Systems, Vol. 12, No. 4, August 2006, 347–362.

Lee, H. et al. (2019). Analysis of steering returnability and compensation logic developmet in limit cornering condition, Int J Automot Technol. 2019; 20 (4): 827-834.

Woo, S. et al. 2019, Control method for electronic limited slip differential, KR:20190042276.

Woo, S. et al. 2019, Control method for electronic limited slip differential, US:16/527,953.

Woo, S. et al. 2018, Estimating method of friction coefficient of road surface for vehicle, KR:20180138771.

Hyundai Motors Company 2020, e-LSD: Electric Limited Slip Differential, IR52 Jang Young-shil Award, 10 WK, 2020, viewed 20 June 2020, <https://www.ir52.com/award/weekly.asp?smenu=award&stitle=weekly&yy=2020&wk=10&jscd=112>.

초   록

전륜 구동 차량의 핸들링 성능을 위한
전자식 차동 제한 장치의 예측 제어 전략

논문은 전륜 구동 차량의 핸들링 및 가속 성능 향상을 위한 전자식 차동 제한 장치, Electronic Limited Slip Differential (ELSD)의 예측 제어 전략에 초점을 맞췄다. 기존 전륜 구동 차는 바퀴에 작은 수직하중으로 선회 내측 구동 휠의 스핀이 발생할 수 있기 때문에 선회 중 가속 시 가속 성능 면에서 불리하고 언더스티어가 과해지는 등 전형적인 단점이 있다. 이 문제를 해결하기 위해 ELSD 에 대한 제어 로직을 제안하여 조종안정성 및 가속 성능을 향상시켰다. 제안된 전자식 차동제한장치 제어 알고리즘은 네 부분으로 구성된다. (1) 선회 중 가속 성능 향상을 위해 언더스티어 방지 로직을 제안하였다. 첫째, 빠른 응답을 위해 휠의 구동 가능 접지력 추정 값의 크기에 따라 선회 내측 및 외측 휠에 구동 토크를 미리 분배한다. 그래도 선회 내측 접지력이 부족하여 휠 스핀이 발생하는 경우, 외측 휠 속도 대비 내측 휠 속도의 초과량에 비례하여 추가 구동 토크를 외측 휠로 전달한다. 다만 외측 휠의 스핀은 절대로 허용하지 않기 위해 비구동 휠 속도 대비 구동 외측 휠 속도의 초과량에 비례하여 외측 휠로의 토크 전달을 제한한다. (2) 오버스티어 방지 로직은 심한 차선 변경 시 과한 요 거동을

96

안정화할 수 있다. 알고리즘은 목표 요 속도 대비 실제 차량의 요 속도 초과량에 비례하여 선회 외측 휠에서 내측 휠로 구동 토크를 전달한다. (3) Electronic Stability Control (ESC) 시스템과의 협조 제어 전략은 구동 토크와 제동 토크의 중복으로부터 ELSD/ESC 시스템을 분리하기 위해 제안되었다. (4) 조향 반력 토크 보상 제어 로직은 좌/우 구동 토크 차이로 인한 토크 스티어 효과를 방지하기 위해 전기식 파워 보조 조향 시스템에 보상 토크를 인가한다. 본 알고리즘은 차량 테스트를 통해 평가되었다. 제안된 알고리즘은 제어 방법과 마찰 추정 방법에 대한 특허를 통해 독창성을 검증 받았다. 그리고 제안된 알고리즘이 적용된 ELSD 는 고성능 양산 차량에 적용되었다. 그 후, ELSD 로 인해 차량 성능 크게 향상된 부분과 관련하여 국외 매체로부터 긍정적인 피드백을 받았다. 또한 제안된 알고리즘이 적용된 시스템은 IR52 장영실상을 수상하여, 기술적 중요성, 독창성, 경제적 가치, 기술적 파급력을 검증 받았다.

주요어: 전자식 차동제한장치, 요 감쇠, 타이어-노면 마찰계수 추정, 휠 스핀, 마찰 원

학　번: 2012-30178